

A MAGNETOAEROELASTIC ENERGY
CONVERSION SCHEME

by

Jerome V. Burchett, Lieutenant, USN

BEE Rensselaer Polytechnic Institute 1959

Submitted in Partial Fulfillment of the

Requirements for the Degrees of

Master of Science in Electrical Engineering

and the

Professional Degree, Naval Engineer

at the

Massachusetts Institute of Technology

(May 1966)

100-100000-100000-100000-100000
100-100000-100000-100000-100000
100-100000-100000-100000-100000

DUDLEY KNOX LIBRARY
NAVAL POSTGRADUATE SCHOOL
MONTEREY CA 93943-5101

A MAGNETOAEROELASTIC ENERGY
CONVERSION SCHEME

by

Jerome Vincent Burchett

BEE Rensselaer Polytechnic Institute
(1959)

Submitted in Partial Fulfillment of the Requirements
for the Degrees of Master of Science

and the

Professional Degree, Naval Engineer

at the

MASSACHUSETTS INSTITUTE OF TECHNOLOGY

June 1966

Signature of Author.....

Department of Naval Architecture

Certified by.....

Thesis Supervisor

Accepted by.....

Chairman, Departmental Committee on Graduate Students

NPS Archive
1966
Burchett, J.

The ~~65~~
B1652

REPORT OF THE NATIONAL HISTORIC LAND ACT

TO THE SECRETARY OF THE INTERIOR

BY

JAMES BURCHETT, JR.

U.S. GEOLOGICAL SURVEY, WASHINGTON, D.C.

(1967)

Submitted to the National Historic Land Act Commission

for the purpose of being included in the list

of National Historic Landmarks

as authorized by the National Historic Land Act

of 1960

and the National Historic Landmark

Act of 1960

Approved for publication by the National Historic Landmark

Commission, Washington, D.C.

Published by the U.S. Geological Survey, Washington, D.C.

1967

U.S. Geological Survey, Washington, D.C.

U.S. Geological Survey, Washington, D.C.

A MAGNETOAEROELASTIC ENERGY CONVERSION SCHEME

by

Jerome Vincent Burchett

Submitted to the Department of Naval Architecture and Marine Engineering on May 20, 1966, in partial fulfillment of the requirements for the Master of Science Degree in Electrical Engineering and the Professional Degree, Naval Engineer.

ABSTRACT

This thesis is a theoretical and experimental study of a scheme for converting energy from a streaming fluid through an elastic plate to an electric circuit. The model is a quasi-one-dimensional motion of the elastic plate under the influence of the supersonic fluid and a transverse magnetic field.

An analysis of the model leads to the equations of motion of the plate in the unrestrained case. By assuming traveling wave solutions, the dispersion relation, resulting from the coupled equations of motion, is solved. The boundary conditions are discussed and the resulting eigenvalue problem is stated. By the method of coupling modes, the effect of the coupling on the wave numbers is determined.

In the experiment, an elastic media is tested for response with electromagnetic and mechanical excitation. The supersonic flow is attained with a set of convergent-divergent nozzles feeding a test section. The combined plate and flow experiment is run and results discussed.

The conclusions are: (1) the theory predicts an instability in the natural modes; (2) the plate can be excited in the second modes and the frequency response increases with tension. (3) The effects of the instability in the combined experiment are masked by forced excitation probably due to the turbulent boundary layer.

Thesis Supervisor: James R. Melcher

Title: Associate Professor of Electrical Engineering

A MATHEMATICAL THEORY
OF ELECTRICITY

by

JAMES CLERK MAXWELL

Submitted to the Department of Natural Philosophy and Astronomy
in partial fulfillment of the
requirements for the degree of Doctor of Philosophy in Natural
Philosophy and the Professional Natural Science.

ABSTRACT

This theory is a mathematical and experimental study of a
medium for the propagation of energy from a vibrating fluid through an
electric space to an electric circuit. The model is a quasi-
dimensional medium of the electric field with the following
the mechanical field and a continuous magnetic field.

Derivatives of the model laws on the question of motion of
the field in the magnetic space. By carrying Maxwell's
equations, the equations of motion, resulting from the coupled
equations of motion, is solved. The boundary conditions are the
constant and the resulting differential problem is treated by the
method of variation of constants, the effect of the coupling on the wave
number is determined.

In the mechanical, an electric field is treated for response
with electrostatic and magnetostatic interaction. The response
time is treated with a set of coupled differential equations
treating a wave packet. The coupled plane and wave equations
is now and results discussed.

The conclusion is: (i) the theory predicts no locality
in the natural motion; (ii) the field can be treated in the natural
motion and the frequency response is treated with locality. (iii) The
effect of the interaction in the mechanical experiment and treated
by second order perturbation theory for the mechanical boundary layer.

These experiments: James C. Maxwell
James Clerk Maxwell on Electrical Dynamics

ACKNOWLEDGMENT

The author wishes to express his appreciation to Professor James R. Melcher for suggesting this project and for his inspiration, guidance and patience during the work of the thesis.

Grateful acknowledgments are also made to Professor Phillip G. Hill and Professor John Dugundji for their suggestions; to Mr. Harold Atlas and Mr. Thorwald Christensen for the experimental assistance, and to Miss Dianne Staples for typing the manuscript.

Much of the numerical work was performed at the Computation Center, Massachusetts Institute of Technology. The experimental portion was supported by the National Aeronautics and Space Administration under NASA Research Grant, NsG-368.

I wish to thank my wife, Donna, for her interest and help during this effort.

The author wishes to express his appreciation to Professor James H. Wilson for suggesting this project and for his assistance and criticism during the work of the 1954.

Mr. [redacted] was also seen at the [redacted] office on [redacted] and [redacted].

Most of the research work was performed at the Department of Physics, Massachusetts Institute of Technology. The experimental results were reported in the Journal of Chemical Physics and the Journal of Chemical Physics.

I wish to thank my wife, Emma, for her interest and help
in this effort.

Table of Contents

Abstract	ii
Acknowledgment	iii
List of Figures	vi
Chapter I Introduction	1
Chapter II Analysis of Device	7
2.1 The Fluid Equations	7
2.2 The Magnetic Equations	9
2.3 The Plate Equations	12
Chapter III The Dispersion Equation	19
Chapter IV Boundary Conditions	30
4.1 A Simple Example	30
4.2 Method of Characteristics	32
4.3 The Eigenvalue Problem	35
4.4 Coupling of Modes	38
4.5 Element Equations	39
4.6 Coupling Between the Elements	42
4.7 Summary	46
Chapter V Experimental Procedure	47
5.1 The Plate Experiments	47
5.2 The Experiment to Obtain Supersonic Flow	52
5.3 An Experiment to Test the Flutter Theory	57
Chapter VI Conclusions and Recommendations	60
6.1 Conclusions	60
6.2 Recommendations	62
Appendix A. A Comparison with Flutter Theory	64
Appendix B. Additional Experimentation	67

LIST OF FIGURES

<u>Figure No.</u>		<u>Page</u>
1.1	A Magnetoaeroelastic Energy Conversion Scheme	2
1.2	Lumped Parameter Model	3
2.1	Analytical Model	8
2.2	Magnetic Circuit	10
2.3	Elastic Plate and Element	13
3.1	Uncoupled Equation	22
3.2	Coupled Equation	25
3.3	Coupled Equation	26
3.4	Coupled Equation	27
4.1	A Membrane Fixed at the Ends	31
4.2	One Dimensional Fluid Flow	34
4.3	Fluid Wave Propagation	34
5.1	Plate Test Section	48
5.2	Plate Tension Versus Frequency	51
5.3	Nozzle Test Section	55
5.4	Pressure Versus Distance in Nozzle	56

Tables

I	Results of Plate Experiment	49
---	-----------------------------	----

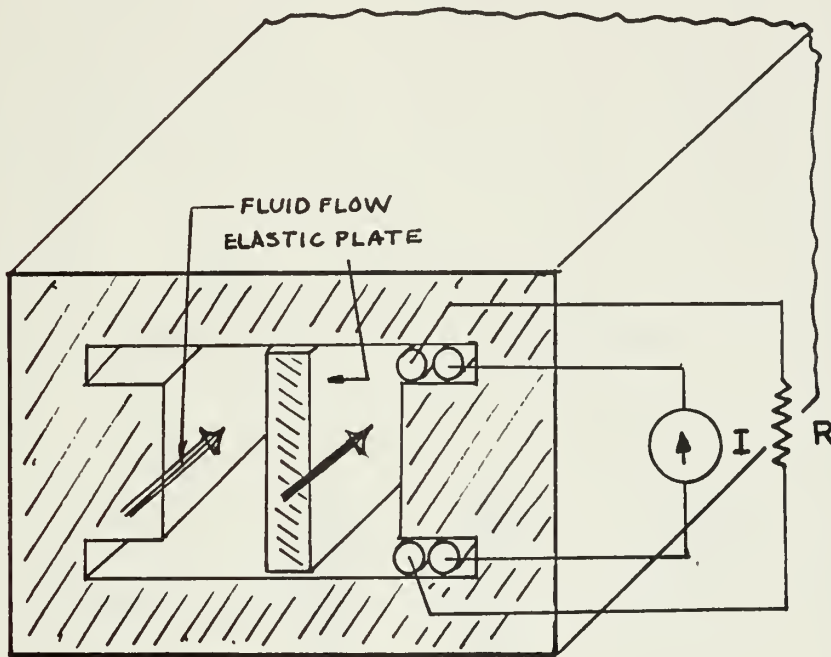
CHAPTER I

Introduction

Energy conversion has historically been accomplished by rotating machinery, making use of small gap lengths and conduction in good conductors. Recent investigations have lead to novel static and dynamic converters. The feasibility of generating d.c. power from the interaction of a moving conducting fluid and an electromagnetic system has already been demonstrated.⁽¹⁾ Several schemes for A.C. power generation have been presented, however, these are restricted by the requirement of large magnetic fields and a good conducting fluid. An alternative method for converting energy is shown in Figure 1.1. It is a device for producing A.C. power by abstracting energy from the fluid flow.

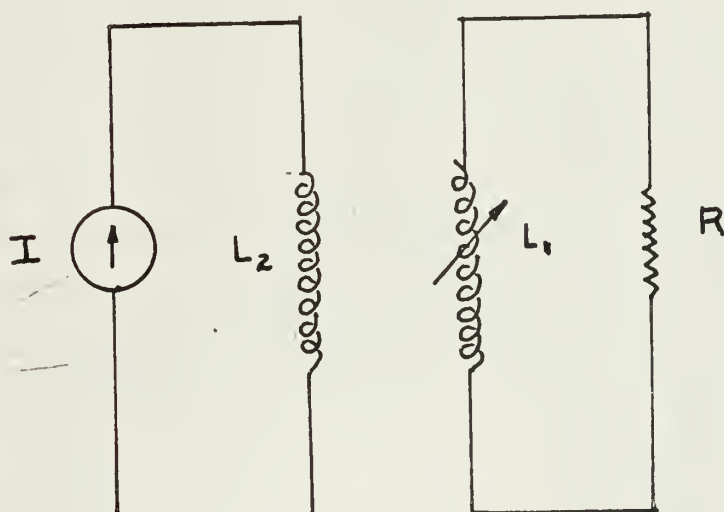
The device consists of an elastic plate in a channel with a fluid flow on both sides. The plate is constructed of highly permeable material and is free to move in the transverse direction. The channel, also of highly permeable material, contains the fluid and copper conductors. One set of conductors is excited by a constant current (D.C.) source, causing a transverse magnetic field. The interaction between the fluid and the plate causes transverse motion of the plate, similar to the "flutter" motion in aero-elasticity. This motion provides a variable coupling of the first circuit with the second magnetic circuit, producing A.C. power, as indicated in the lumped parameter model shown in Figure 1.2.

Analytically the problem of the thin airfoil performing small lateral oscillations in a uniform stream of incompressible fluid



A MAGNETOAEROELASTIC ENERGY CONVERSION SCHEME

FIGURE 1.1



LUMPED PARAMETER
MODEL

FIGURE 1.2

was for many years the heart of all flutter prediction. The complete solution was first published in the United States by Theodorsen⁽²⁾. This approach has been further developed by many workers and is presented most comprehensively in the text, Aeroelasticity, by Bisplinghoff, etc.⁽³⁾

The definition of panel flutter is the self excited oscillation of the external skin of a flight vehicle when exposed to an airflow on one side. The analysis of panel flutter has been pursued in great detail recently, but there is still some disagreement between theory and experiment. It appears that the theoretical considerations to date do not approach the situation described here. The tensions on the panel are significantly less than those to be applied in this device. The mechanism for flutter is not explained physically in the context of a feedback situation. However, the effects of aspect ratio, elastic foundations, damping and boundary support have been covered in detail. In the appendix a comparison of the prediction of flutter theory and the predictions of this theory is shown. The aeroelastician in general has confined his analysis to that of "infinite" flow, whereas in this scheme the confining effect of the rigid walls will be important. In dense fluids, there has also been investigation of flow induced vibrations of fla

follow:

recent

elastic.^(5,6) The latter is concerned with a statistical representation of the turbulent boundary layer as a forcing function. Here again, the models have infinite geometry and, therefore, are not directly applicable. Lastly there are several "handbook" solutions available for determining natural modes of vibration, for

and is presented more comprehensively in the text. Synopsis,
by Alphonse, etc.⁽⁷⁾

There are many years the heart of all that nation. The con-
viction solution was first applied in the United States by them.

induced vibrations of the

[illegible]

example, see Den Hertog ⁽⁷⁾.

Melcher ⁽⁸⁾ has studied field coupled surface waves for both electrohydrodynamic and magnetohydrodynamic systems. Ketterer, ⁽⁹⁾ studying under him, investigated the interactions between a fluid stream and a fixed structure capable of supporting traveling waves. By theory and experiment, it was shown that energy could be extracted from the flow in the form of oscillations.

In this study there is contact between the fluid and the elastic structure which was not present in the experiment conducted by Ketterer. The effect of this contact, a boundary layer which could be turbulent, may be considerable in comparison to the effect of an instability in the natural modes.

There are several methods of exciting the plate available. First, it could be located transversely in the flow path, similar to holding a piece of grass between the thumbs and blowing. However, the length of interaction would be limited and therefore, the amount of energy taken from the flow would be limited. Secondly, the plate could be fixed at one end only, and the excitation would be dependent on the trailing vortices. This would be similar to the study reported by Eagleson. ⁽⁴⁾ Another method that has been suggested is to place the plate in a tube closed at the downstream end and put the combination in the supersonic flow. This would provide greater excitation since pressure variations considerably above stagnation pressure have been observed in such a configuration. The overall efficiency of this scheme is questionable, however.

The method chosen was considered both theoretically and experi-

resonance, and the system (7).

Below (8) are similar trials comparing system wave for both electrohydrodynamic and magnetohydrodynamic systems. In this section, we have investigated the relationship between a fluid system and a fluid structure capable of supporting traveling waves. In theory and experiment, it was shown that energy could be extracted from the flow in the form of oscillations.

In this study, there is a direct relationship between the fluid and the elastic structure which was not present in the experiment conducted by Fletcher. The effect of this contact, a secondary layer, could be considered, but be responsible in contrast to the effect of an instability in the primary layer.

There are several methods of exciting the plate oscillations. First, it could be located externally in the flow field, which is to hold a plate of fluid between the tanks and driving. However, the length of excitation would be limited and therefore, the amount of energy taken from the flow would be limited.

Secondly, the plate could be fixed at one end only, and the other end would be free to oscillate. This would be similar to the study reported by Fletcher, (1967) which showed that the plate would be in a low class of the spectrum and not in the condition in the spectrum. This would provide greater excitation since pressure variations continuously above resonance frequency have been observed in such a configuration. The overall efficiency of this scheme is quite limited, however.

The system chosen was considered both theoretically and experimentally. The system was chosen to be a fluid system in which the fluid is in contact with the structure.

CHAPTER II

mentally the simplest to study, with the added feature that the significant interaction length might produce a reasonably efficient device. In Chapter II, the device is studied by assuming a quasi-one dimensional motion of the plate. The resulting dispersion relationship is solved in Chapter III and the implications discussed. In chapter IV the longitudinal boundary conditions are treated. The experiment and results are described in Chapter V.

It is desirable to note at this point that the objective is a device that can be excited in a microwave. The proposed optimization will also allow calculation the effects of gravity. The fluid flow, the plate and the magnetic effects will be treated separately, and then the results will be combined to obtain the equations of motion.

2.1 The Fluid Equations

In the bulk of the fluid, if body forces are neglected, the equations are:

$$\rho \frac{\partial u}{\partial t} = - \frac{\partial p}{\partial x} \quad (2.1)$$

For an incompressible fluid and the equation for continuity of mass is

$$\frac{\partial u}{\partial x} + \frac{\partial v}{\partial y} = 0 \quad (2.2)$$

The continuity equation will require some consideration and that the above are then compared to the fluid flow equations, and so on.

CHAPTER II

ANALYSIS OF DEVICE

The device will be modeled by assuming a quasi-one dimensional motion of the plate. The model, as seen in cross-section from a top view, is shown in Figure 2.1. The flow will be assumed inviscid and incompressible in this analysis since the objective is a device that can be tested in a wind-tunnel. The proposed orientation will also allow neglecting the effects of gravity. The fluid flow, the plate and the magnetic effects will be treated separately, and then the results will be combined to obtain the equations of motion

2.1 The Fluid Equations:

In the bulk of the fluid, if body forces are neglected, the momentum equation is

$$\rho \frac{Du_i}{Dt} + \frac{\partial p}{\partial x_i} = 0 \quad (2.1)$$

for an inviscid fluid and the equation for continuity of mass is

$$\frac{D\rho}{Dt} + \rho \nabla \cdot \mathbf{u}_i = 0 \quad (2.2)$$

FIGURE 2.1

for compressible flow. We will assume small perturbations and that the waves are long compared to the significant dimensions, that is:

CHAPTER 11

ANALYSIS OF BEAMS

The device will be useful in analyzing a continuous beam-
 along motion of the plate. The model is continuous
 from one view, is shown in figure 1. The film will be removed
 instead not unnecessary in this analysis when an object
 is a device that can be tested in a wind-tunnel. The proposed
 operation will also allow detecting the effects of gravity.
 The fluid film, the plate and the supports which will be tested
 separately, and then the results will be compared to obtain the
 equivalent of motion

11.1 The Fluid Boundary

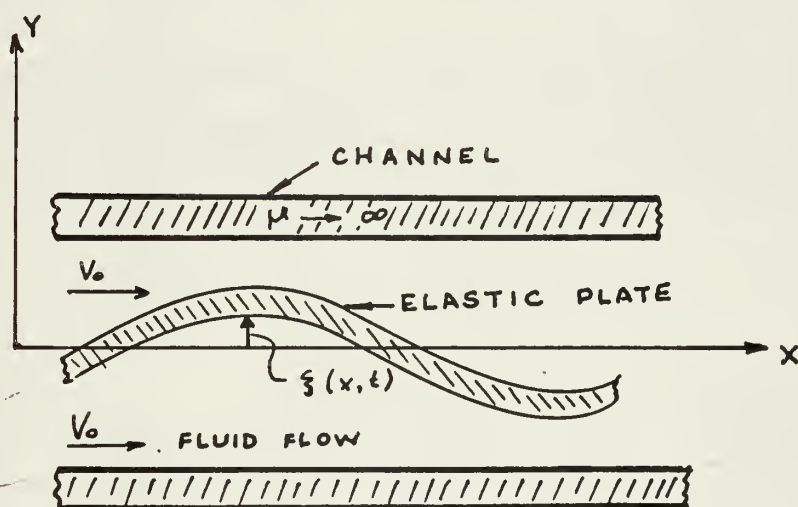
In the case of the fluid, it may be assumed that the
 momentum equation is

$$\rho \frac{d^2 y}{dt^2} = - \frac{\partial p}{\partial y}$$

For an inviscid fluid and the equation for continuity of mass is

$$\frac{\partial \rho}{\partial t} + \rho \frac{\partial y}{\partial t} = 0$$

For compressible flow the total energy will be conserved and
 that the mass is conserved in the absence of sources,
 that is



ANALYTICAL MODEL

FIGURE 2.1

$$v_x = v'_x(x,t) - v_o$$

$$v'_y = v_y(x,t)$$

$$p(x,t) = p'(x,t) - p_o \ll p_o$$

$$\rho(x,t) = \rho'(x,t) - \rho_o \ll \rho_o$$

where the primed quantities are the actual values and the unprimed quantities the perturbations. Inserting these into equations (2.1) and (2.2) and retaining only first order terms:

$$\rho_o \left(\frac{\partial v_x}{\partial t} + v_o \frac{\partial v_x}{\partial x} \right) + \frac{\partial p}{\partial x} = 0 \quad (2.3)$$

$$\rho_o \left(\frac{\partial v_x}{\partial x} + \frac{\partial v_y}{\partial y} \right) + \left(\frac{\partial}{\partial t} + v_o \frac{\partial}{\partial x} \right) \rho = 0 \quad (2.4)$$

Initially, the thermodynamic process will be considered adiabatic, which allows relating the changes in pressure and density by a constant.

$$\partial p = C^2 \partial \rho$$

FIGURE 2.2

2.2 Magnetic Equations

A section of the magnetic circuit is shown in Figure 2.2. We assume a perfectly magnetic material so that the coil will induce a magnetic field in the circuit, with the H field existing

$$\frac{\partial}{\partial t} \left(\frac{\partial \psi}{\partial x} \right) = \frac{\partial}{\partial x} \left(\frac{\partial \psi}{\partial t} \right)$$

$$\frac{\partial}{\partial t} \left(\frac{\partial \psi}{\partial x} \right) = \frac{\partial}{\partial x} \left(\frac{\partial \psi}{\partial t} \right)$$

$$\frac{\partial}{\partial t} \left(\frac{\partial \psi}{\partial x} \right) = \frac{\partial}{\partial x} \left(\frac{\partial \psi}{\partial t} \right)$$

$$\frac{\partial}{\partial t} \left(\frac{\partial \psi}{\partial x} \right) = \frac{\partial}{\partial x} \left(\frac{\partial \psi}{\partial t} \right)$$

where the terms in parentheses are the actual values and the approx-
 imations are the approximations. The terms in parentheses are the actual
 values and the terms in parentheses are the approximations.

$$\frac{\partial}{\partial t} \left(\frac{\partial \psi}{\partial x} \right) = \frac{\partial}{\partial x} \left(\frac{\partial \psi}{\partial t} \right)$$

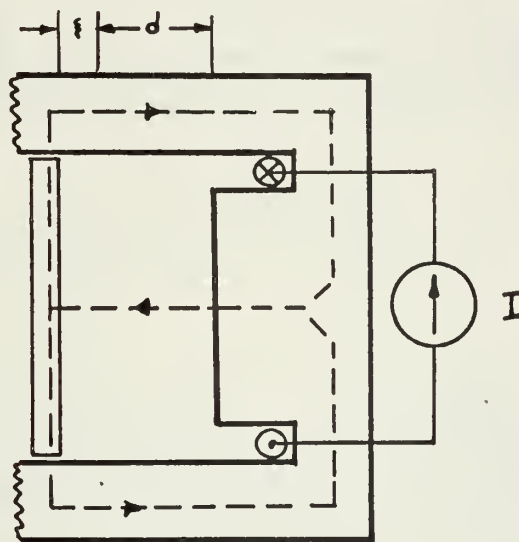
$$\frac{\partial}{\partial t} \left(\frac{\partial \psi}{\partial x} \right) = \frac{\partial}{\partial x} \left(\frac{\partial \psi}{\partial t} \right)$$

Initially, the control system will be considered as a
 system which will be considered as a system which will be considered
 as a system.

$$\frac{\partial}{\partial t} \left(\frac{\partial \psi}{\partial x} \right) = \frac{\partial}{\partial x} \left(\frac{\partial \psi}{\partial t} \right)$$

2.2. Magnetic Field

A section of the magnetic circuit is shown in Figure 2.2.
 We assume a perfectly magnetic material so that the field will
 induce a magnetic field in the circuit, with the field being



MAGNETIC CIRCUIT

FIGURE 2.2

in the gap only. From Ampere's circuital law we get:

$$\oint \mathbf{H} \cdot d\mathbf{l} = \int_{\text{gap}} \mathbf{H} \cdot d\mathbf{l} = NI$$

$$\text{or } H = \frac{NI}{d+\xi} = \frac{NI}{d} \left(\frac{1}{1+\xi/d} \right)$$

Define: $H_0 = \frac{NI}{d}$ as the steady state H field. Therefore, the magnetic fields with reference to figure (2.1) will be:

Therefore, the force is proportional to the displacement and will have the effect of the plate.

$$H_y = H_0 \left(\frac{1}{1+\xi/d} \right)$$

where the superscripts refer to the respective sides of the plate. There are several methods available for computing the force on the plate. The most direct method is to use the Maxwell Stress Tensor described in detail in reference. (8) The force density in the y direction acting on the plate is the sum of the stresses acting in that direction on each of the faces of the plate. The stress tensor:

$$\tau_{ij} = \mu H_i H_j - \frac{\mu}{2} \delta_{ij} H_k H_k$$

In our case, where H_y is the only significant component, this becomes

$$\tau_{yi} = \frac{\mu}{2} H_y^2$$

in the gas only. From Amundsen's experimental law we get:

$$\left\{ \begin{aligned} \Delta H_{\text{gas}} &= \Delta H_{\text{liq}} - RT \end{aligned} \right.$$

$$\text{or } \Delta H_{\text{gas}} = \Delta H_{\text{liq}} - \frac{RT}{\Delta T} \left(\frac{1}{T_1} - \frac{1}{T_2} \right)$$

Defining $\Delta H_{\text{gas}} = \Delta H_{\text{liq}} - \frac{RT}{\Delta T}$ as the standard state ΔH_{liq} . Therefore, the magnetic field also depends on temperature (T) will be:

$$\Delta H_{\text{gas}} = \Delta H_{\text{liq}} - \frac{RT}{\Delta T} \left(\frac{1}{T_1} - \frac{1}{T_2} \right)$$

where the superscript refers to the respective sides of the film. There are several methods available for measuring the force on the plate. The most direct method is to use the known force exerted by the plate in a liquid in vacuum.⁽¹⁷⁾ The force density in the y direction acting on the plate is the sum of the pressure acting in that direction on each of the faces of the plate. The stress tensor:

$$\tau_{ij} = \rho \frac{\partial u_i}{\partial x_j} = \rho \frac{\partial u_j}{\partial x_i}$$

in our case, where ρ is the only significant component this becomes

$$\tau_{ij} = \rho \frac{\partial u_i}{\partial x_j}$$

and the force per unit area is

$$f_y = \frac{\mu}{2} H_o^2 \left(\frac{1}{(1+\xi/d)^2} - \frac{1}{(1-\xi/d)^2} \right)$$

Keeping only the linear terms, the force density is simply:

$$f_y = 2\mu_o H_o^2 \frac{\xi}{d}$$

Therefore, the force is proportional to the displacement and will have a destabilizing effect on the plate.

2.3 The Plate Equation

The plate has a density ρ and a modulus of elasticity E . Using simple beam theory, the bending moment at any point is proportional to the rate of change of the slope.

$$m = \frac{EI}{w} \frac{\partial^2 \xi}{\partial x^2} \quad \text{and} \quad dm = \frac{EI}{w} \frac{\partial^3 \xi}{\partial x^3} dx$$

Taking an elemental section as in Figure 2.3, we can indicate all of the forces and moments acting on it.

ELASTIC PLATE AND ELEMENT

$$f = \text{external force density} = 2\mu_o H_o^2 \frac{\xi}{d} + (p^u - p^l)$$

v = shear force per unit width.

p = tensile force per unit width.

and the force per unit area is

$$f = \frac{1}{2} \rho v^2 \left(1 - \frac{1}{(1 + \frac{1}{2} \rho v^2)^2} \right)$$

keeping only the linear terms. The force density is thereby

$$f = \frac{1}{2} \rho v^2$$

Therefore, the force is proportional to the displacement and will have a characteristic period of the plate,

2.2 The plate equation

The plate has a density ρ and a modulus of elasticity E . Using simple beam theory, the bending moment at any point is proportional to the rate of change of the slope,

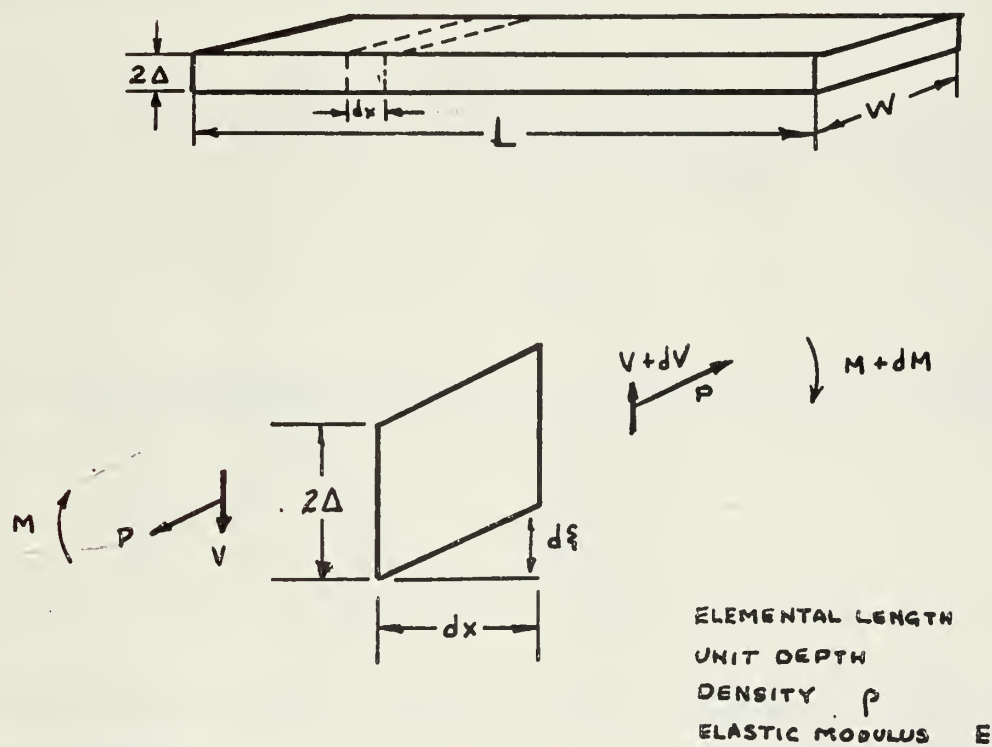
$$M = \frac{E I}{L} \frac{dy}{dx} \quad \text{and} \quad \frac{dM}{dx} = \frac{E I}{L} \frac{d^2 y}{dx^2}$$

Taking an elemental section as in Figure 2, we can determine all of the forces and moments acting on it.

$$F = \text{external force density} = \frac{E I}{L} \frac{d^2 y}{dx^2}$$

where F is the force per unit width.

$q = \text{external force per unit width}$



ELASTIC PLATE AND ELEMENT

FIGURE 2.3

m = bending moment.

Now, summing the moments about the lower left hand corner:

The shear stress and velocity must be zero at the channel walls
in both the upper and lower regions

$$-dm - vdx + p d\xi = 0 \quad \text{or}$$

$$v = -\frac{dm}{dx} + p \frac{d\xi}{dx} = -\frac{EI}{w} \frac{d^3 \xi}{dx^3} + p \frac{d\xi}{dx}$$

and the forces acting on the element.

If $f + \frac{dv}{dx} = \rho m 2 \Delta \frac{\partial^2 \xi}{\partial t^2}$ or
equal the plate velocity at the plate

$$f + p \frac{d^2 \xi}{dx^2} - \frac{EI}{w} \frac{d^4 \xi}{dx^4} = \rho m 2 \Delta \frac{\partial^2 \xi}{\partial t^2} \quad (2.5)$$

The three previous developments can be combined to give the equations of motion.

2.4 The Equations of Motion

Equation (2.4) can be rearranged and integrated directly.

$$-\frac{\partial v}{\partial y} = \frac{1}{\rho_o c^2} \left(\frac{\partial}{\partial t} + v_o \frac{\partial}{\partial x} \right) p + \frac{\partial v}{\partial x}$$

$$-v_y = \left(\frac{1}{\rho_o c^2} \left(\frac{\partial}{\partial t} + v_o \frac{\partial}{\partial x} \right) p + \frac{\partial v_x}{\partial x} \right) (y) \Big|_1^2 \quad (2.6)$$

The transverse fluid velocity must be zero at the channel wall in both the upper and lower regions:

$$-v_y^u = \left(\frac{1}{\rho_o c^2} \left(\frac{\partial}{\partial t} + v_o \frac{\partial}{\partial x} \right) p^u + \frac{\partial v_x}{\partial x} \right) (y \pm a) \quad (2.7)$$

If one assumes no cavitation the transverse fluid velocity must equal the plate velocity at the plate.

$$-v_y^u(y = +\Delta + \xi) = \left(\frac{1}{\rho_o c^2} \left(\frac{\partial}{\partial t} + v_o \frac{\partial}{\partial x} \right) p^u + \frac{\partial v_x}{\partial x} \right) (\Delta + \xi - a)$$

$$-v_y^l(y = -\Delta + \xi) = \left(\frac{1}{\rho_o c^2} \left(\frac{\partial}{\partial t} + v_o \frac{\partial}{\partial x} \right) p^l + \frac{\partial v_x}{\partial x} \right) (-\Delta + \xi + a)$$

Since the perturbation ξ is small, $(\Delta + \xi - a) = -d$ and $v_y^u(y = \Delta + \xi) = \frac{\partial \xi}{\partial t} + v_o \frac{\partial \xi}{\partial x}$,

the above two equations maybe added:

$$2 \left(\frac{\partial \xi}{\partial t} + v_o \frac{\partial \xi}{\partial x} \right) = \left(\frac{1}{\rho_o c^2} \left(\frac{\partial}{\partial x} + v_o \frac{\partial}{\partial x} \right) (v_x^u - v_x^l + \frac{\partial}{\partial x} (p^u - p^l)) \right) d \quad (2.8)$$

Equation (2.7), the plate equation, maybe rearranged and inserted in (2.3) and (2.8) to eliminate $(p^u - p^l)$, the pressure difference, from our equations:

$$\frac{\partial}{\partial x} \left(2\mu H_o^2 \frac{\xi}{d} - \frac{EI}{w} \frac{\partial^4 \xi}{\partial x^4} + p \frac{\partial^2 \xi}{\partial x^2} - 2\rho m \Delta \frac{\partial^2 \xi}{\partial t^2} \right) + \rho_o \left(\frac{\partial}{\partial t} + v_o \frac{\partial}{\partial x} \right) v = 0 \quad (2.9)$$

$$\left(\frac{\partial}{\partial t} + v_o \frac{\partial}{\partial x} \right) \xi - \frac{d}{2\rho_o c^2} \left(\frac{\partial}{\partial t} + v_o \frac{\partial}{\partial x} \right) \left(2\mu_o H^2 \frac{\xi}{d} - \frac{EI}{w} \frac{\partial^4 \xi}{\partial x^4} + p \frac{\partial^2 \xi}{\partial x^2} \right.$$

$$\left. - 2\rho m \Delta \frac{\partial^2 \xi}{\partial t^2} \right) - \frac{d}{2} \frac{\partial}{\partial x} v = 0 \quad (2.10)$$

where we have defined $v = (v_x^u - v_x^l)$.

It will be convenient to have the equations in nondimensional form before further manipulations:

Variables: $\eta = \xi/d$, $v = \frac{v}{v_o}$, $\bar{x} = x/d$, $\bar{k} = kd$, $\bar{\omega} = \omega \frac{d}{v_o}$, $\bar{t} = \frac{v_o}{d} t$

Parameters: $\mu = \frac{\rho_o d}{\rho_m \Delta}$, density ratio,

$M_a = \frac{c}{v_o}$, Fluid "Mach" number

$M_m = \frac{(P/2\Delta\rho_m)^{1/2}}{v_o}$, Material "Mach" number

$H = \frac{\mu_o H^2 d}{\rho_m v_o^2 \Delta}$, Magnetic pressure

$D = \frac{EI}{w 2 \rho_m v_o^2 d^2 \Delta}$, Rigidity

We have normalized the parameters to a dynamic pressure $(\frac{1}{2} \rho v_o^2)$ and then multiplied by the density ratio. This will simplify the solutions as well as provide an indication of the strength of the various forces or pressures compared to the fluid dynamic pressure.

We now multiply equation (2.9) by $\frac{d \rho_o c^2}{\Delta \rho_m v_o^2}$ and equation (2.10)

We have normalized the data points to a common constant $(\frac{1}{2} \pi \sqrt{\epsilon})$ and then plotted the localities. This will clearly show relations as well as provide an indication of the strength of the various forms of pressure compared to the fluid pressure.

by $\frac{d^2}{2\Delta\rho_m v_o^2}$:

$$\mu M_a^2 \left(\frac{\partial}{\partial \bar{t}} + \frac{\partial}{\partial \bar{x}} \right) \eta - \left(\frac{\partial}{\partial \bar{t}} + \frac{\partial}{\partial \bar{x}} \right) (H-D \frac{\partial^4}{\partial \bar{x}^4} + M_m^2 \frac{\partial^2}{\partial \bar{x}^2}) \eta - \frac{\mu}{2} M_a^2 \frac{\partial}{\partial \bar{x}} v = 0$$

(2.11)

$$\frac{\partial}{\partial \bar{x}} (H-D \frac{\partial^4}{\partial \bar{x}^4} + M_m^2 \frac{\partial^2}{\partial \bar{x}^2} - \frac{\partial^2}{\partial \bar{t}^2}) \eta + \frac{\mu}{2} \left(\frac{\partial}{\partial \bar{t}} + \frac{\partial}{\partial \bar{x}} \right) v = 0$$

(2.12)

The above form the equations of motion of the system in nondimensional form.

To solve these equations as they stand for specified forcing function would be difficult indeed. This approach has been followed on simplified equations, where the forcing function was a statistical representation of the boundary layer excitation. The approach we will follow is to look for instabilities in the free modes, when the source of oscillations is not a lossy one as it is in a turbulent boundary layer.

$$p = \frac{1}{2} \frac{1}{\sqrt{1 - \frac{v^2}{c^2}}}$$

(11.1)

(12.1)

The above form for the expression of the action is convenient for the calculation of the

invariant mass of the system. To obtain the invariant mass of the system, we first calculate the invariant mass of the system, which is the sum of the invariant masses of the particles. The invariant mass of the system is given by the expression

is the invariant mass of the system.

CHAPTER III

THE DISPERSION EQUATION

The dispersion equation, or the relationship between $\bar{\omega}$ and \bar{k} , will give an indication of the stability of the plate in the free modes. We will assume a delta function in time and space as the excitation, so that the equation of motion will have no driving function. In order to determine whether the structure can support traveling waves, we also assume that the solutions will be of the form $\eta = \hat{\eta} e^{j(\omega t - kx)}$ and $v = \hat{v} e^{j(\omega t - kx)}$. Inserting these into the equations of motion we get:

$$(\bar{\omega} - \bar{k}) (\mu M_a^2 - H + D\bar{k}^4 + M_m^2 \bar{k}^2 - \bar{\omega}^2) \hat{\eta} + \frac{\mu}{2} (M_a^2 \bar{k}) \hat{v} = 0 \quad (3.1)$$

$$-\bar{k} (H - D\bar{k}^4 - M_m^2 \bar{k}^2 + \bar{\omega}^2) \hat{\eta} + \frac{\mu}{2} (\bar{\omega} - \bar{k}) \hat{v} = 0 \quad (3.2)$$

Setting the determinant of the coefficients equal to zero will insure that the equations of motion are compatible:

$$-\frac{\mu}{2} \{ (\bar{\omega} - \bar{k})^2 (\mu M_a^2 - H + D\bar{k}^4 + M_m^2 \bar{k}^2 - \bar{\omega}^2) + M_a^2 \bar{k}^2 (H - D\bar{k}^4 - M_m^2 \bar{k}^2 + \bar{\omega}^2) \} = 0 \quad (3.3)$$

CHAPTER 12

THE BIVARIATE COVARIANCE

The dispersion equation or the relationship between \bar{Y} and \bar{X} will give an indication of the possibility of the data in the line model. We will assume a linear function in time and space as the expectation, so that the relation of \bar{Y} and \bar{X} will have no direct connection. In order to determine whether the structure and the part traveling waves, we also assume that the principle will be of the form $\bar{Y} = \bar{X} + \bar{Z}$ (see Fig. 12.1). The \bar{Z} is the error term, and the \bar{X} is the mean of the \bar{Y} and \bar{X} (see Fig. 12.2).

$$\bar{Y} = \bar{X} + \bar{Z} \quad (12.1)$$

$$\bar{Y} = \bar{X} + \bar{Z} \quad (12.2)$$

(12.3)

Letting the dispersion of the covariance wave in time will insure that the dispersion of the wave is constant.

$$\bar{Y} = \bar{X} + \bar{Z} \quad (12.4)$$

This is the desired dispersion relationship, and its solution, $\bar{\omega} = f(\bar{k})$, and the inverse, $\bar{k} = f(\bar{\omega})$, will provide insight into the stability of the infinite plate. Before proceeding with the solution, there are several limiting cases which should be investigated. These in effect will separate the two systems.

1) If we allow the tension, P , on the plate to become infinite, the plate becomes a rigid boundary.

Thus, if $M_m \rightarrow \infty$, we get:

$$(\bar{\omega} - \bar{k})^2 \bar{k}^2 + M_a^2 \bar{k}^2 (-\bar{k}^2) = 0$$

or, in dimensional form:

$$(\omega - V_0 k)^2 = M_a^2 k^2 \quad (3.4)$$

which is the expected dispersion equation for convective acoustic waves

2) Similarly if we allow the density of the fluid to approach zero, we find the equation of the plate alone.

$$\bar{\omega}^2 = -H + D\bar{k}^4 + M_m^2 \bar{k}^2 \quad (3.5)$$

This is the desired dispersion relationship, and for solution, $\bar{n} = \bar{n}(\bar{k})$, and one obtains, $\bar{k} = \bar{k}(\bar{n})$, with \bar{n} and \bar{k} both functions of the wave number \bar{k} . In the limit where $\bar{n} \rightarrow \infty$, the solution, there are no waves. In the case where $\bar{n} \rightarrow 0$, there is a limit where the two systems.

If we allow the system, \bar{n} , to take on values, the above relation is valid.

Then, if $\bar{n} \rightarrow \infty$, we have

$$\bar{k} = \bar{k}(\bar{n}) = \bar{k}(\infty) = \bar{k}(\infty)$$

or, in the limit $\bar{n} \rightarrow \infty$

$$\bar{k} = \bar{k}(\infty) = \bar{k}(\infty)$$

(3.4)

which is the desired dispersion relation for non-relativistic waves.

3) Similarly, if we allow the density \bar{n} to approach zero, we find the dispersion relation for the case where

(3.5)

$$\bar{k} = \bar{k}(\bar{n}) = \bar{k}(\infty) = \bar{k}(\infty)$$

It is comforting to note that the magnetic force will have a destabilizing effect, while the tension and rigidity tend to stabilize the solution.

3) Allowing the speed of sound to become infinite will restrict the solution to the subsonic region. In dimensional form:

$$2\mu H^2 \frac{\xi}{d} - \frac{EI}{w} \frac{\partial^4 \xi}{\partial x^4} + P \frac{\partial^2 \xi}{\partial x^2} - 2\rho m \Delta \frac{\partial^2 \xi}{\partial t^2} + 2\rho_o V_o^2 \frac{\xi}{d} = 0$$

This is the equation for the plate with a dynamic pressure term which can be derived from Bernoulli's equation in a linearized form (assuming $\frac{\partial}{\partial t} \rightarrow 0$)

$$P_o + \frac{1}{2} \rho_o V_o^2 = P + \frac{1}{2} \rho \left(\frac{V_o d}{d - \xi} \right)^2 = P_o + P' + \frac{1}{2} \rho V_o^2 + \rho V_o^2 \frac{\xi}{d}$$

then:

$$P' - P'' = 2\rho_o V_o^2 \frac{\xi}{d}$$

The above three checks indicate that the model and the analysis are consistent. It also appears that they are to some extent physical. UNCOUPLLED EQUATIONS

The third check gives a static instability which has been observed at subsonic speeds. (10)

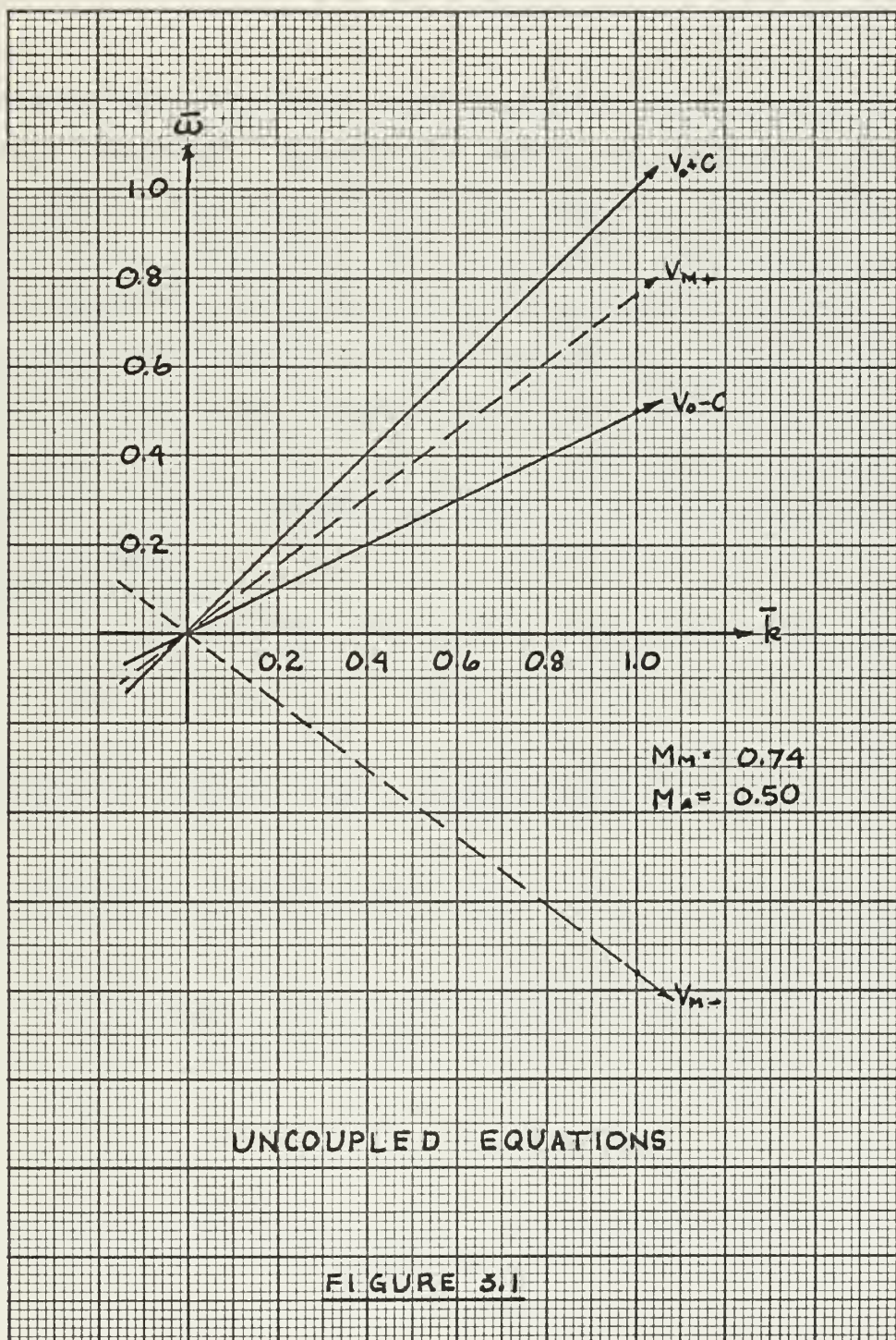
The uncoupled equations (3.4) and (3.5) can be solved simply, since they are quadratic, and plotted, as in Figure 3.1. For the

It is considered to have been the dominant force of the 19th century, while the 20th century was dominated by the rise of the state.

This is the equation for the space with a dynamic boundary condition which can be derived from Hamilton's equations in a discretized form (see eq. (2) → 7).

levels are consistent. It also means that they are to some extent ethical.

The unpaired electrons (3.4) and (3.5) can be solved directly since they are quadratic and linear, as in Figure 3.1. For the



rest of the analysis, some experimental considerations will govern the approach. Supersonic speeds are difficult to attain, and in general, the experimental apparatus is designed for a specified flow. Therefore, we will take V_0 to be a constant equal to twice the speed of sound. The rigidity of the plate is also a fixed quantity for a given experiment and the effect of its variation would be roughly equivalent to varying the tension on the plate. Since the plate tension is easily changed experimentally, it will be allowed to vary in the solution of the dispersion equation.

We now rearrange the dispersion equation as a polynomial in $\bar{\omega}$:

$$\bar{\omega}^4 + \bar{\omega}^3 (-2\bar{k}) + \bar{\omega}^2 (H - D\bar{k}^4 - M_m^2 \bar{k}^2 - M_a^2 - \bar{k}^2 M_a^2 + \bar{k}^2)$$

$$+ \bar{\omega} (2\bar{k}) (-H + D\bar{k}^4 + M_m^2 \bar{k}^2 + M_a^2)$$

$$+ (-\bar{k}^2) (M_a^2 - 1) (H - D\bar{k}^4 - M_m^2 \bar{k}^2) = 0$$

(3.6)

and, using the computer, solve for real values of \bar{k} .

rest of the analysis, some experimental considerations will govern the approach. Economic models are difficult to design and in general, the experimental technique is limited for a specified flow. Therefore, we will take $\frac{1}{2}$ of the constant equal to twice the speed of sound. The velocity of the fluid is also a fixed quantity for a given experiment and the effect of its variation would be roughly equivalent to varying the length on the plate. Since the plate length is easily changed experimentally, it will be allowed to vary in the solution of the two-region equation.

We now reexamine the hypothesis of selection as a determinant of

and, using the constant, solve for μ and σ .

The results are shown in Figures 3.2, 3.3, and 3.4 for the following cases:

- | | | |
|---------------|--------------|------------------|
| 1) Figure 3.2 | $M_m = .875$ | (strong tension) |
| 2) Figure 3.3 | $M_m = .545$ | (medium tension) |
| 3) Figure 3.4 | $M_m = .314$ | (weak tension) |

The solutions plotted in Figure 3.1 remain as the asymptotes for these solutions. Returning to equations 3.3 and 3.4, we find in dimensional form:

$$\omega = (V \pm c)k \quad \text{for the fluid}$$

$$\omega = \pm \left(\frac{p}{\rho} \right)^{1/2} k \quad \text{for the plate}$$

In the case of strong tension the coupling is weak. However, as the tension is decreased as in Figure 3.3 to a point where (v_{mt}) , the wave speed in the plate, is approximately equal to $(V-c)$, the "slow" fluid wave, the coupling becomes pronounced. Decreasing the tension further, decreases the coupling until the solutions are uncoupled.

The two systems, the fluid and the plate, are in themselves stable at at least if the magnetic field is small. The above solutions indicate that when coupled together an unstable situa-

The results are shown in Figures 2.2, 2.3, and 2.4 for the following cases:

- 1) Figure 2.2 $\gamma = 0.5$ (strong coupling)
- 2) Figure 2.3 $\gamma = 0.25$ (medium coupling)
- 3) Figure 2.4 $\gamma = 0.15$ (weak coupling)

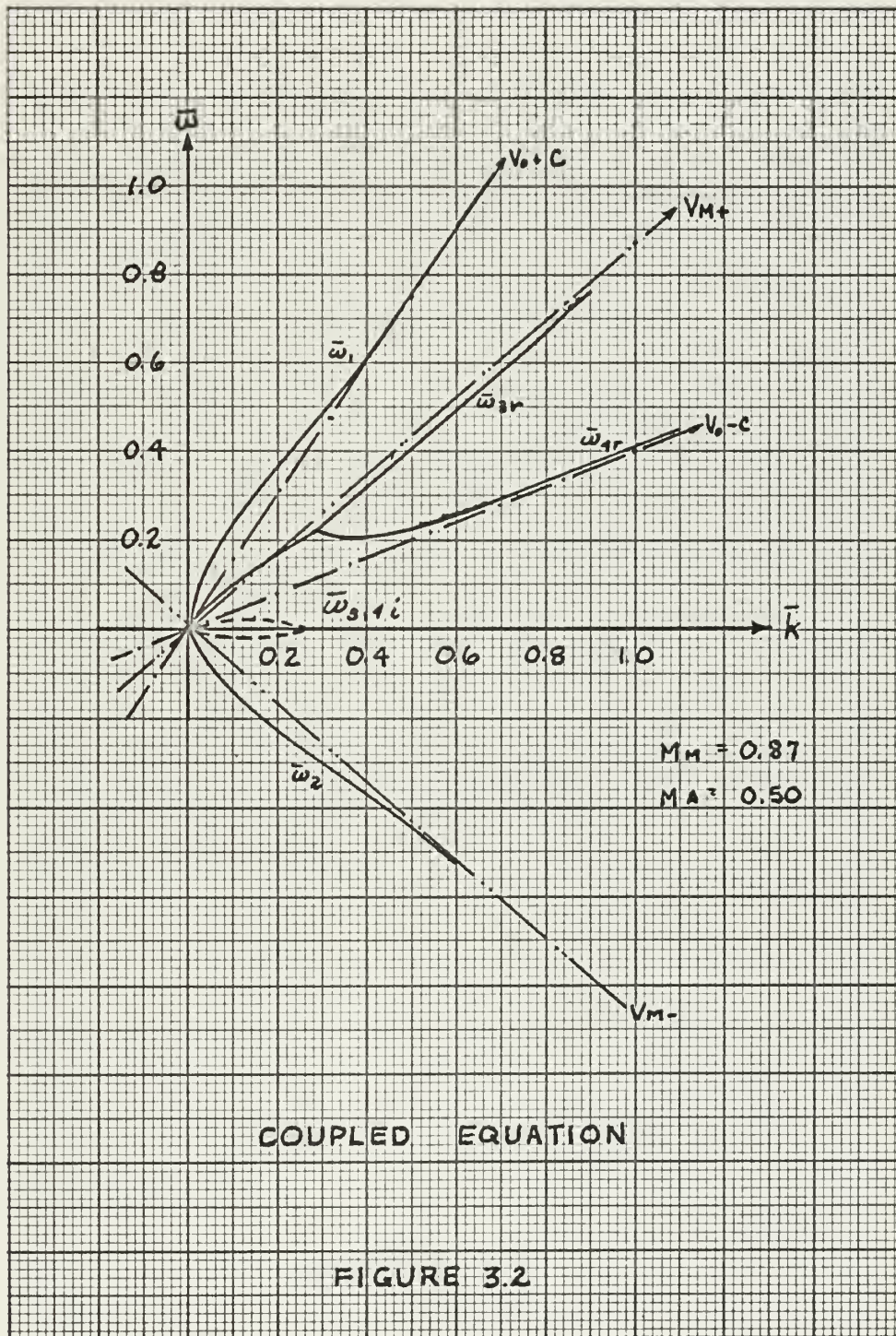
The solutions plotted in Figure 1.1 remain in the physical region for these solutions. According to equations 1.2 and 1.6, the field in dimensional form

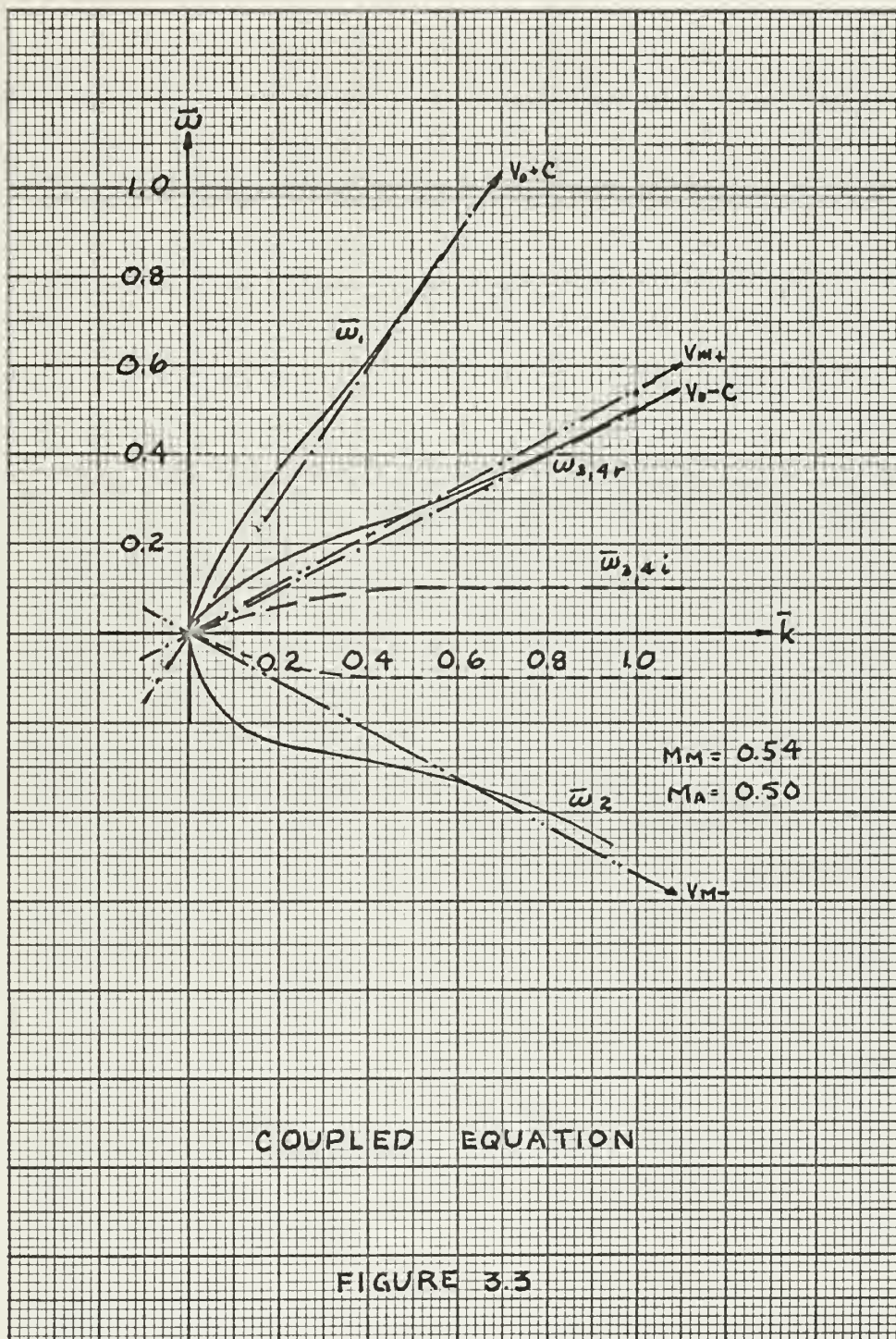
$$\omega = (V\sigma)^2 \quad \text{for the field}$$

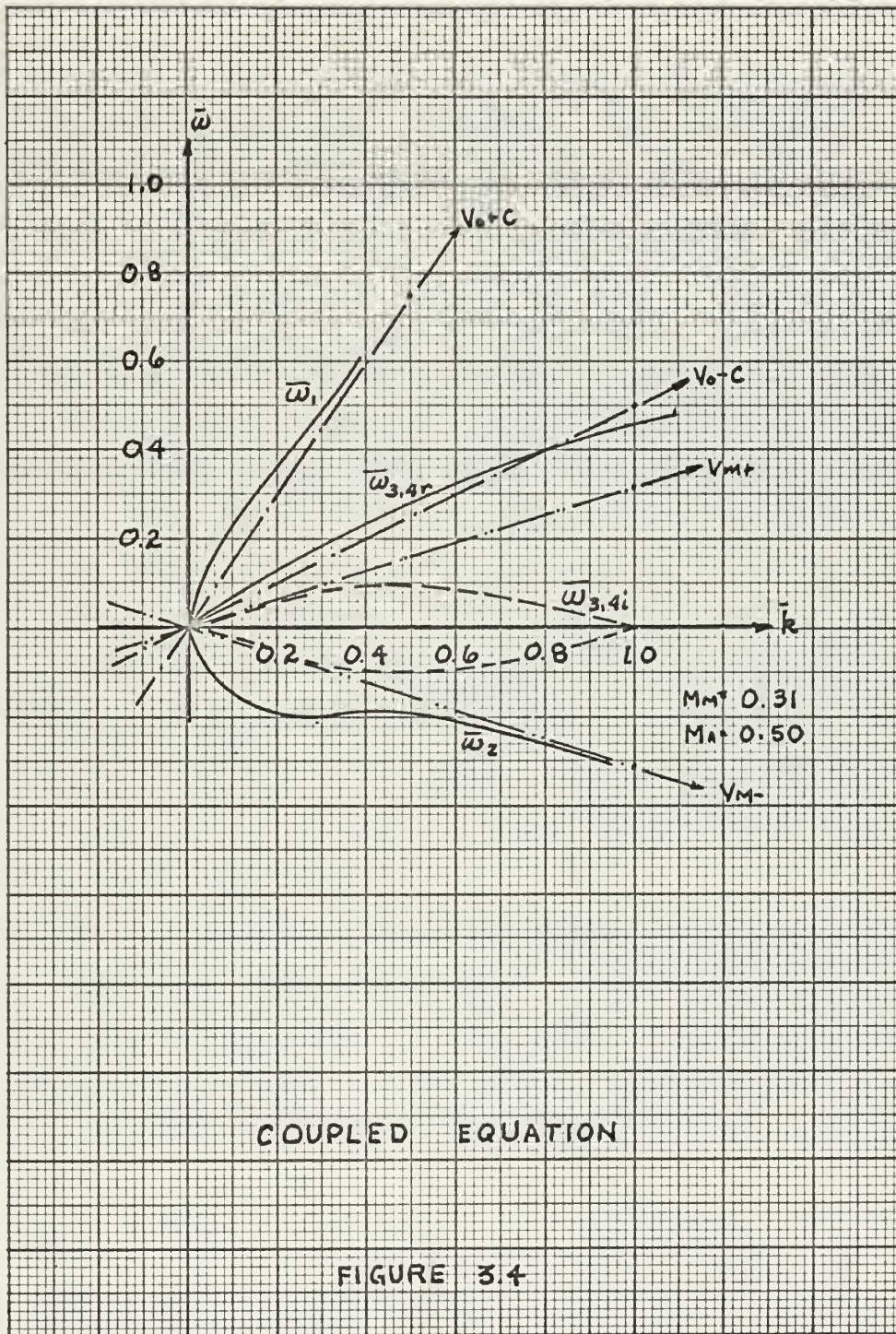
$$\omega = \frac{1}{2} \left(\frac{g}{V} \right)^2 \quad \text{for the wave}$$

In the case of strong coupling the coupling is weak. However, as the tension is decreased as in Figure 1.1 to a value where $\omega_{\text{min}} < \omega_{\text{max}}$, the wave speed in the shock, is approximately equal to $(V\sigma)^2$. The "slow" limit, the coupling becomes stronger, decreasing the tension further, however the coupling will still be strong and remains.

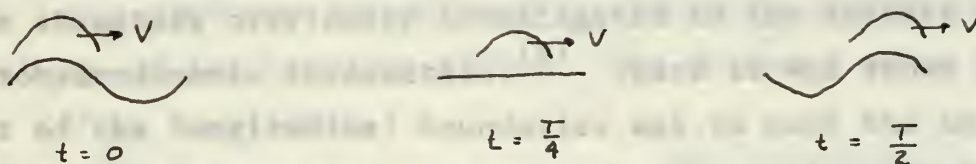
The two systems, the field and the wave, are in equilibrium stable at least in the neighborhood of ω_{min} . The wave solutions indicate that when coupled together an unstable situation







tion is produced. That is: $\bar{\omega}$ has a negative imaginary part and the assumed solution: $n = n_0 e^{j(\omega t - kx)}$ has the form: $n = n_0 e^{at + j(\omega t - kx)}$ such that the displacement grows in time. This is the result of a feedback mechanism within the coupled system. Let's assume a deflection of the plate in the second mode, with a positive amplitude over the leading half of the plate. This provides a compression wave in the fluid. As this disturbance is swept downstream, it arrives over the trailing half of the plate in time to reinforce the motion of plate. Then the motion is transmitted

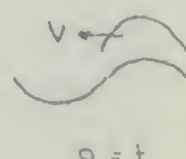
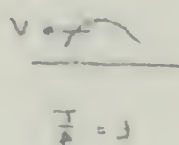
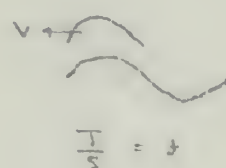


back upstream through the plate, to arrive at the right time to start the procedure over again. This is the case when the velocities V_{m+} and $V-c$ are equal. Since this is a distributed phenomenon over the half length of the plate, the mechanism will work for velocities that are approximately equal as well as exactly equal.

A complete discussion of the dispersion equation as it pertains to the infinite problem would not add significantly to the study of the device proposed. However, the steps will be outlined.

tion is produced. That is, \bar{u} has a negative frequency and the assumed solution $u_{\text{ass}} = A e^{i(\omega t - kx)}$ has the form $u = 0$ such that the displacement grows in time. This is the result of a feedback mechanism within the coupled system. The average deflection of the plate in one second mode, with a positive amplitude over the leading half of the plate. This provides a compression wave in the fluid. As this displacement is sent downstream, it arrives over the trailing half of the plate in time to reinforce the motion of plate. Then the motion is trans-

mitted



back upstream through the fluid, to arrive at the right time to start the procedure over again. This is the case when the velocities V_{up} and V_{down} are small. When this is a distributed phenomenon over the half length of the plate, the mechanism will work for velocities that are sufficiently small as well as exactly

equal

A complete discussion of the dispersion mechanism as it pertains to the infinite medium would not add significantly to the study of the device proposed. However, the above will be sufficient

Having solved for $\bar{\omega} = f(\bar{k}_{\text{real}})$, the complex values of $\bar{\omega}$ obtained are substituted and the equation solved for $k_r + jk_i = f(\omega_r + j\omega_i)$ to determine the type of instability involved. This can be done using the Bers-Briggs criteria,⁽¹¹⁾ with the help of computer technique giving a graphical display of both ω_r versus ω_i and k_r versus k_i as described by Mills.⁽¹²⁾

The dispersion equations shown in Figures 3.2 - 3.4 have characteristics which indicate that the basic theoretical model is physically meaningful. The coupling between the flow and the elastic media occurs at long wave lengths, with the short wavelengths stable and uncoupled. These are the properties of the stream structure previously investigated in the context of an electrohydrodynamic interaction.⁽⁸⁾ There it was shown that the effect of the longitudinal boundaries was to make the instability absolute. That is, the theory supports the conjecture that growing oscillations can be produced.

Consider a uniform flow of the fluid. This is similar to the elastic state of the fluid and the fluid is uniform.

1. Equation of motion:

$$\frac{\partial^2 \psi}{\partial t^2} = - \frac{\partial^2 \psi}{\partial x^2}$$

2. Assume solution of the form: $\psi = A \sin k_x x + B \cos k_x x$

3. Transverse deflection: $\psi = y(x) e^{j\omega t}$

having solved for $\bar{u} = 10^6$ the constant value of \bar{u} obtained are substituted and the equation solved for $\bar{u} = 10^6$ and $\bar{u} = 10^7$ to determine the type of instability involved. This can be done using the beta-beta criteria, which the ratio of conductivities giving a physical picture of both \bar{u} versus \bar{u} and \bar{u} versus \bar{u} as described by Miller (1971).

The dispersion equation shown in Figure 2.2 - 2.4 have characteristics which indicate that the beta-beta instability is physically unstable. The coupling between the slow and the elastic media occurs at long wave lengths, with the short wave-lengths stable and unexcited. These are the conditions of the stream structure previously investigated in the context of the electrodynamic interaction. (1971) There is also shown that the effect of the localized boundary was to make the instability absolute. That is, the theory predicts the instability that grows long oscillations can be described.

The stream structure shown in Figure 2.2 - 2.4 have characteristics which indicate that the beta-beta instability is physically unstable. The coupling between the slow and the elastic media occurs at long wave lengths, with the short wave-lengths stable and unexcited. These are the conditions of the stream structure previously investigated in the context of the electrodynamic interaction. (1971) There is also shown that the effect of the localized boundary was to make the instability absolute. That is, the theory predicts the instability that grows long oscillations can be described.

The stream structure shown in Figure 2.2 - 2.4 have characteristics which indicate that the beta-beta instability is physically unstable. The coupling between the slow and the elastic media occurs at long wave lengths, with the short wave-lengths stable and unexcited. These are the conditions of the stream structure previously investigated in the context of the electrodynamic interaction. (1971) There is also shown that the effect of the localized boundary was to make the instability absolute. That is, the theory predicts the instability that grows long oscillations can be described.

CHAPTER IV

BOUNDARY CONDITIONS

The application of the boundary conditions will be approached by two methods, an exact method resulting in the eigenvalue problem and an approximate method called the coupling of modes approach. A simple linearized example will be covered first followed by a discussion of how to apply the boundary conditions. This leads to the statement of the eigenvalue problem. Next, the coupling of modes is discussed. This will give an indication of a more meaningful way of applying the boundary conditions, and an estimate of the coupling effect. The boundary value problem is not solved completely.

TENSILE STRESS - P
DENSITY - ρ

4.1 A Simple Example

Consider a membrane fixed at the ends. This is similar to the elastic plate if the rigidity and the fluid are neglected.

A MEMBRANE FIXED AT THE ENDS

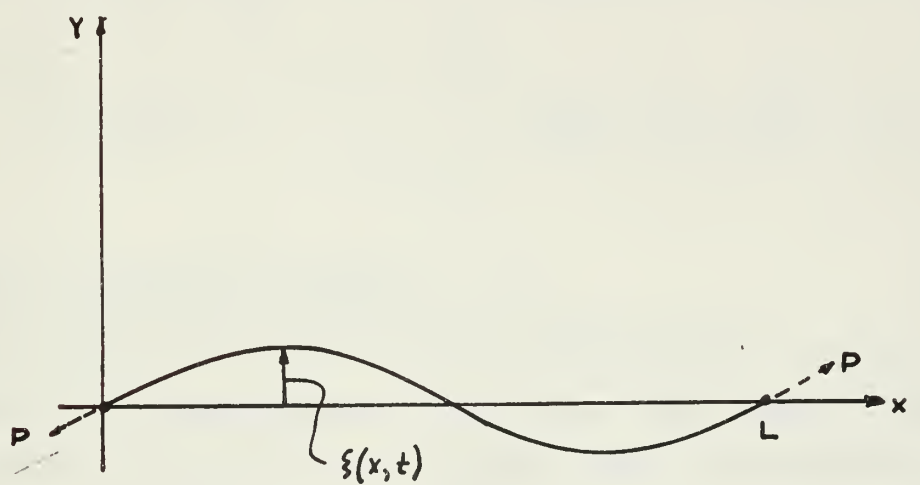
- 1 Equations of motion:
$$\rho \frac{\partial^2 \xi}{\partial t^2} = P \frac{d^2 \xi}{dx^2}$$
- 2, Assume Solutions of the form: $\xi = (A \sin k_x + B \cos k_x) e^{j\omega t}$
3. Dispersion Relationship: $\omega^2 = P/\rho k^2$

FIGURE 4.2

is not solved completely. The boundary value problem and estimate of the coupling stress. The boundary value problem and estimate of the coupling stress. The boundary value problem and estimate of the coupling stress.

the classic effect of the electric and gas fluid are explained.

5. Assume \mathcal{B} is a Boolean algebra. Let $f: \mathcal{B} \rightarrow \mathcal{B}$ be a function. Define f^* to be the function $f^*: \mathcal{B} \rightarrow \mathcal{B}$ defined by $f^*(x) = f(x^*)$. Prove that f^* is a function.



TENSILE STRESS - P
DENSITY - ρ

A MEMBRANE FIXED AT THE ENDS

FIGURE 4.1

4. Boundary Conditions:

$$1) \quad \xi(0,t) = 0 \quad B = 0$$

$$2) \quad \xi(L,t) = 0 \quad A \sin kL = 0 \quad \text{and} \quad k = \frac{n\pi}{L}$$

5. Solution:

$$\xi(x,t) = \text{Re} \left\{ \left(A_n \sin \frac{n\pi x}{L} \right) e^{j \left(\left(\frac{p^2}{c} \right) \frac{n\pi}{L} \right) t} \right\}$$

4.2. Method of Characteristics

In the example the basic steps to the problem solution are stated. There is a significant change when the fluid is added, especially when it is allowed to have a gross translational motion. The question arises - at what point may one apply boundary conditions on the flow such that they are meaningful? Were the fluid motionless, the boundary conditions must be applied at two points in space. This is also true if the velocity of the fluid is less than the speed of sound in the fluid. From the dispersion equation, however, the instabilities occur at supersonic speeds only.

In order to understand this more clearly, the method of characteristics is useful. This method uses the general solutions of the wave equation for the transient case:

$$f = f_+ (x-ct) + f_- (x+ct)$$

4. Boundary Conditions

$$f(t, x) = 0 \quad x = 1$$

$$f(t, x) = 0 \quad x = 0 \quad \frac{\partial f}{\partial x} = 0 \quad x = 0$$

5. Solution:

$$\left\{ f(t, x) = \sum_{n=0}^{\infty} \frac{1}{n!} \left(\frac{\partial^n f}{\partial x^n} \right)_{x=0} \right.$$

6. Method of Characteristics

In the example the basic ideas to the general solution are stated. There is a slight change when the fluid is solid, especially when it is allowed to have a gross deformation motion. The question arises - is there any and how? boundary conditions on the flow such that they are meaningful? Now the fluid motionless, the boundary conditions must be applied at two points in space. This is also true if the velocity of the fluid is less than the speed of sound in the fluid. From the operation equation, however, the initial value is not at two points speeds only.

In order to understand this more clearly, the method of characteristics is useful. This method uses the general solution of the wave equation for the transient case.

$$f = f + (x - ct) + f - (x + ct)$$

where f^+ is a wave propagating in the plus x direction and f^- a wave in the negative x direction. The solutions are represented by the third dimension of a graph where the first two are time and space. Thus a disturbance can be followed in both time and space.

Let : $\alpha = x + ct$ and $\beta = x - ct$

FIGURE 4.2

Assume a disturbance: $p = P_0 - a < x < +a$

$= 0$ elsewhere.

for the fluid flow shown in Figure 4.2.

In Figure 4.3 the disturbance is shown.

Lines representing constant α and β can be drawn on the graph. Those originating at $x = \pm a$ are the most interesting since they show the progress of the disturbance. For example, at $t = t_0$ the position of the disturbance can be determined from:

$$f = f^+(\beta) \quad t = t_0 + f^-(\alpha) \quad t = t_0$$

The slope of the lines is of interest since, if the lines of β had a positive slope, the point $x = -L$, would never know the disturbance. This is the case when the fluid is allowed to have motion at a velocity greater than the speed of sound. For a translating media, we must redefine:

FLUID WAVE PROPAGATION

$$\alpha = x + (v+c)t \quad \text{and} \quad \beta = x + (v-c)t$$

FIGURE 4.3

space. Thus a disturbance can be followed in each case and space by the third dimension of a graph where the first two are time and wave in the negative x direction. The equations are transformed where $4x$ is a wave propagating in the x direction and $4t$ is

$$3\pi - \pi = 2 \text{ (area)} \quad 2\pi + \pi = 3\pi \quad : 36.1$$

Annals of Mathematics

For the third time shown in Figure 4.7.

in France A. S. the Government of France

[illegible]

$$g^{-1} = 3 \quad f(1-3) = g^{-1} = 3 \quad f(3) = 1$$

motion at a velocity greater than the speed of sound. For a trans-

$$d(\text{day})/\text{hr} = 0 \quad 600 \quad 3(5\text{hr})/2 \approx 7.5$$

600

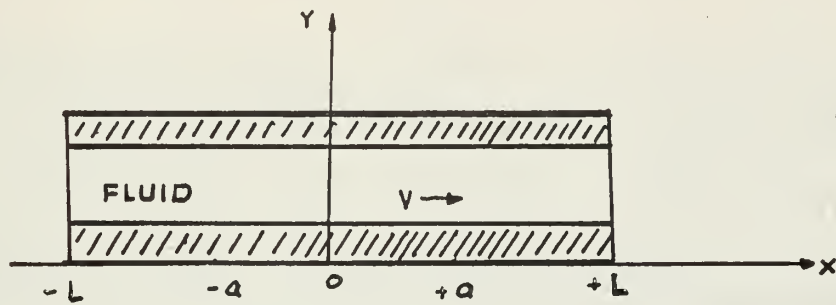
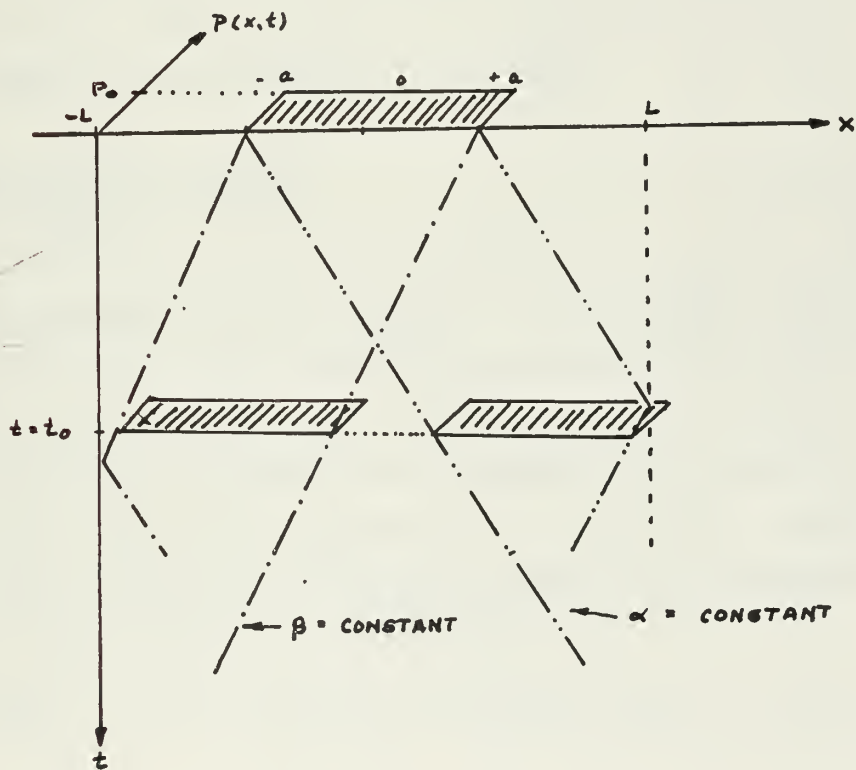


FIGURE 4.2



FLUID WAVE PROPAGATION

FIGURE 4.3

as the characteristic solutions to the convecting wave equation. Then $(v-c)$, the slope of the β lines, becomes positive for $v > c$, and points upstream will not be effected by events downstream.

This implies, in the scheme proposed, that the fluid boundary conditions must be applied at the leading edge of the plate in order to determine their effect on the interaction. The fluid will not know what is happening at the trailing edge until it gets there. There are two variables on the flow, the pressure and velocity, and their values at the point $x = 0$, as a function of time, form the constraints on the flow.

4.3 The Eigenvalue Problem

The dispersion equations was sixth order in $\bar{\omega}$. The six boundary conditions are the two specified for the flow, plus the four on the plate. From simple beam theory the latter are determined from the type of support-free, pinned, or clamped. If we assume the ends are clamped, this implies that that the deflection and slope, $\frac{d\xi}{dx}$, are zero at $x = 0$ and $x = L$. Since $v(x,t)$ and $p(x,t)$ are defined as difference quantities (above and below the plate), their values are zero at $x = 0$.

Returning to the equations of motion this can be stated simply.

$$(\bar{\omega} - \bar{k})(\mu Ma - P.E.) \hat{\eta} + \frac{\mu}{2} (Ma^2 \bar{k}^2) \hat{v} = 0 \quad (4.1)$$

$$\bar{k}(P.E.) \hat{\eta} + \frac{\mu}{2} (\bar{\omega} - \bar{k}) \hat{v} = 0 \quad (4.2)$$

as the characteristic surfaces in the neighborhood of the origin, then (v-c), the slope of the ψ lines, becomes positive for $v > 0$, and points upstream will not be affected by small disturbances.

This implies, in the system proposed, that the limit boundary conditions must be applied at the leading edge of the plate in order to determine their effect on the integration. The fluid will not know what is happening at the leading edge until it gets there. There are two variables on the line, the stream function and velocity, and their values at the point $x = 0$, are a function of time, for the constants on the flow.

§3 The Eigenvalue Problem

The dispersion equation was first given in §2. The six boundary conditions are the two specified on the line, plus the four on the plate. From shape laws about the plate we determined from the type of singularities, pinches, or cusps. If we assume the ends are rounded, then we assume that the behavior of the ends is like $\frac{1}{x^2}$. The same at $x = 0$ and $x = L$. Then $\psi(x, 0)$ and $\psi(x, L)$ are defined as difference quotients (above and below the plate), their values are zero at $x = 0$.

Substituting in the equations of motion this can be stated as

(3.1)

$$(3.1) \quad \psi(x, 0) = \psi(x, L) = 0 \quad \text{and} \quad \psi(0, y) = \psi(L, y) = 0$$

$$(3.2) \quad \psi(0, y) = \psi(L, y) = 0 \quad \text{and} \quad \psi(x, 0) = \psi(x, L) = 0$$

$$(P.E.)\eta + p = 0 \quad (4.3)$$

$$\text{where } P.E. = H - Dk^2 - M_m^2 k^2 + \omega^2$$

As in the example, assume a solution of the form:

$$\eta(x,t) = \text{Re} \left\{ \sum_n A_n e^{-jk_n x} e^{j\omega_n t} \right\}$$

and rewrite equation (4.1) and (4.2).

$$p = - \frac{1}{P.E.} \eta \quad (4.4)$$

$$v = \frac{\mu}{2} \frac{(\omega - \bar{k})}{\bar{k}(P.E.)} \eta = f_1 \eta \quad (4.5)$$

applying the boundary conditions:

$$(1) \quad \eta(0,t) = 0 \quad \sum A_n = 0 \quad (4.6a)$$

$$(2) \quad \frac{\partial \eta}{\partial x}(0,t) = 0 \quad \sum jk_n A_n = 0 \quad (4.6b)$$

$$(3) \quad \eta(L,t) = 0 \quad \sum A_n e^{jk_n L} = 0 \quad (4.6c)$$

$$(4) \quad \frac{\partial \eta}{\partial x}(L,t) = 0 \quad \sum 2jk_n A_n e^{jk_n L} = 0 \quad (4.6d)$$

$$(5) \quad p(0,t) = 0 \quad \sum 2 \left(- \frac{1}{(P.E.(k_n))} \right) A_n = 0 \quad (4.6e)$$

(1.2)

$$u = v + w \quad (1.2)$$

As in the example, assume a solution of the form

$$u(x, y, z) = \sum_{n=1}^{\infty} A_n \sin \frac{n\pi x}{a} \sin \frac{n\pi y}{b} \sin \frac{n\pi z}{c} \quad (1.3)$$

and substitute equation (1.3) into (1.2)

(1.4)

$$v = \frac{1}{2} \left(\frac{1}{a} + \frac{1}{b} + \frac{1}{c} \right) \quad (1.4)$$

(1.5)

$$v = \frac{1}{2} \left(\frac{1}{a} + \frac{1}{b} + \frac{1}{c} \right) \quad (1.5)$$

Applying the boundary conditions:

(1.6)

$$u(0, y, z) = 0 \quad (1.6)$$

(1.7)

$$u(x, 0, z) = 0 \quad (1.7)$$

(1.8)

$$u(x, y, 0) = 0 \quad (1.8)$$

(1.9)

$$u(x, y, c) = 0 \quad (1.9)$$

(1.10)

$$u(0, y, z) = 0 \quad (1.10)$$

$$(6) \quad v(0, t) = 0 \quad \sum 2f_1(k_n) A_n = 0 \quad (4.6f)$$

5.3 Method of Coupling of Modes

Rearranging in matrix form:

$$\Delta(\bar{\omega}, \bar{k}) = 0$$

$$\begin{bmatrix} 1 & 1 & 1 & 1 & 1 & 1 \\ \bar{k}_1 & \bar{k}_2 & \bar{k}_3 & \bar{k}_4 & \bar{k}_5 & \bar{k}_6 \\ e^{j\bar{k}_1 L} & e^{j\bar{k}_2 L} & e^{j\bar{k}_3 L} & e^{j\bar{k}_4 L} & e^{j\bar{k}_5 L} & e^{j\bar{k}_6 L} \\ \bar{k}_1 e^{j\bar{k}_1 L} & \bar{k}_2 e^{j\bar{k}_2 L} & \bar{k}_3 e^{j\bar{k}_3 L} & \bar{k}_4 e^{j\bar{k}_4 L} & \bar{k}_5 e^{j\bar{k}_5 L} & \bar{k}_6 e^{j\bar{k}_6 L} \\ -\frac{1}{\text{P.E.}(\bar{k}_1)} & -\frac{1}{\text{P.E.}(\bar{k}_2)} & -\frac{1}{\text{P.E.}(\bar{k}_3)} & -\frac{1}{\text{P.E.}(\bar{k}_4)} & -\frac{1}{\text{P.E.}(\bar{k}_5)} & -\frac{1}{\text{P.E.}(\bar{k}_6)} \\ f_1(\bar{k}_1) & f_1(\bar{k}_2) & f_1(\bar{k}_3) & f_1(\bar{k}_4) & f_1(\bar{k}_5) & f_1(\bar{k}_6) \end{bmatrix}$$

In theory then the equations $\Delta(\bar{\omega}, \bar{k}) = 0$ and $D(\bar{\omega}, \bar{k}) = 0$ can be solved. Assuming a complex ω , the six k 's are found from $D(\omega, k) = 0$. These values are substituted in to Δ . This procedure is continued until $\Delta = 0$; both it's real and imaginary parts, since it is complex. In practice another method, that of weak coupling of modes will be used to attack the problem.

4.4 Method of Coupling of Modes

One might ask the question: "If two systems are individually stable, why would a weak coupling between the two result in totally different motions?" The answer is that the basic solutions for the two systems are approximately correct, and that the changes can be predicted within certain limitations. First, the systems must be stable by themselves. In this problem, this restriction will not allow including the effect of the magnetic stress on the plate since it has destabilizing influence. Secondly, the coupling between the two systems must be weak. Within these restrictions, mutual coupling of modes will allow simplifications based on a physical understanding of the system.

In theory, the approach is quite simple.⁽¹³⁾ A complicated system is first divided into its component parts. The equations of motion for the isolated systems are solved exactly, and the solutions are expressed in the "normal modes" of the element. The complex system is then assumed to be made up of these elements weakly coupled. The motions within the system are described by the elemental motions which are slightly perturbed by the coupling.

As an example, in the system under consideration the elemental parts are the fluid and the plate. Assuming the fluid motionless and the plate of negligible rigidity (a membrane), each will propagate disturbances as waves, both a forward wave and a backward wave in each system. As seen from the solution

2.4 Method of Variation of Modes

One might ask the question: "If two systems are individually stable, why would a weak coupling between the two result in totally different motions?" The answer is that the basic equations for the two systems are approximately correct, and that the changes can be predicted with certain limitations. First, the systems must be stable by themselves. In this problem, this condition will not allow including the effect of the magnetic fields on the plasma since it has destabilizing influence. Secondly, the coupling between the two systems must be weak. Within these restrictions, mutual coupling of modes will allow simplifications based on a physical understanding of the system.

In theory, the system is quite simple (13). The equations are first divided into its component parts. The equations of motion for the isolated systems are solved exactly, and the solutions are expressed in the normal modes of the system. The complex system is then assumed to be made up of these elements weakly coupled. The motions within the system are described by the elemental motions which are slightly perturbed in the coupling.

As an example, in the system under consideration the elemental parts are the fluid and the plate. Assuming the fluid motions and the plate to negligible rigidly (a membrane), each will propagate disturbances as waves, both a forward wave and a backward wave in each system. As seen from the solution

of the dispersion relationship, the coupling will occur between the forward membrane wave and the "backward" fluid wave. Therefore, the other two waves can be neglected. The motion of the system will be that of these two waves slightly altered by the coupling.

4.5 Elemental Equations in the Coupled Mode Form

1. Fluid Equations

The fluid equations can be greatly simplified to get an approximation to the solution.

$$\frac{\partial v(x,t)}{\partial x} = - \frac{1}{\rho_0(v+c)} \frac{\partial p(x,t)}{\partial t} \quad (4.8a)$$

$$\frac{\partial p(x,t)}{\partial x} = -\rho_0 \frac{\partial v(x,t)}{\partial t} \quad (4.8b)$$

These coupled equations are most easily solved if a method of decoupling them can be found. Following, Louisell,⁽¹³⁾ the decoupled form is derived from linear combinations of the above equations. That is; assume a normal mode form:

$$b_{\pm}(x,t) = \frac{1}{2} (\rho) \left(v(x,t) + \frac{1}{\rho_0(v+c)} p(x,t) \right)$$

of the dispersion relationship, the coupling will result between the forward and backward modes and the backward mode will be lost, the other two modes can be neglected. The system of the system will be that of those two modes already derived for the coupling.

4.2.2. Fundamental Equations in the Coupled Mode Form

4.2.2.1. Coupled Equations

The coupled equations can be exactly simplified to give an approximation for the solution.

$$(4.2a) \quad \frac{d}{dx} \begin{pmatrix} a_1 \\ a_2 \end{pmatrix} = \begin{pmatrix} \beta_1 & \kappa \\ \kappa^* & \beta_2 \end{pmatrix} \begin{pmatrix} a_1 \\ a_2 \end{pmatrix}$$

$$(4.2b) \quad \frac{d}{dx} \begin{pmatrix} b_1 \\ b_2 \end{pmatrix} = \begin{pmatrix} \beta_1 & \kappa \\ \kappa^* & \beta_2 \end{pmatrix} \begin{pmatrix} b_1 \\ b_2 \end{pmatrix}$$

These coupled equations are most easily solved if a method of decoupling them can be found. Following [1], the decoupled form is derived from linear combinations of the above equations. That is, assume a normal mode form:

$$a_1 = \frac{1}{2} (A + B) e^{i(\beta_1 x + \beta_2 z)} + \frac{1}{2} (A - B) e^{i(\beta_1 x - \beta_2 z)}$$

where the mode amplitudes are normalized so that the square of the amplitudes represents energy carried by the mode.

Multiplying equation (4.8b) by the fluid impedance $(\frac{1}{\rho_0(v \pm c)})$ and adding and subtracting from equation (4.8a) will give the desired decoupled form:

$$\frac{\partial}{\partial x} (v \pm \frac{1}{\rho_0(v \pm c)} p) = - \frac{1}{v \pm c} \frac{\partial}{\partial t} (v \pm \frac{1}{\rho_0(v \pm c)} p)$$

or

$$\frac{\partial}{\partial x} (b \pm (x, t)) = - \frac{1}{v \pm c} \frac{\partial}{\partial t} (b \pm (x, t))$$

Assume that the time dependence will be of the form $e^{j\omega t}$,

then: $b \pm (x, t) = a \pm (x) e^{j\omega t} + a_{\pm}^*(x) e^{-j\omega t}$

Now if $v(x, t) = \text{Re } \bar{v}(x) e^{j\omega t}$

then $a \pm (x) = \frac{1}{2} (\rho)^{\frac{1}{2}} (\bar{v}(x) + \frac{1}{\rho_0(v \pm c)} \bar{p}(x))$

and equations (4.8a) and (4.8b) become

$$(\frac{\partial}{\partial x} + jk) a_+(x) = 0 \quad (\frac{\partial}{\partial x} - jk) a_+^*(x) = 0 \quad (4.9a)$$

$$(\frac{\partial}{\partial x} - jk) a_-(x) = 0 \quad (\frac{\partial}{\partial x} + jk) a_-^*(x) = 0 \quad (4.9b)$$

the amplitude necessary to excite the nodes, while the nodes amplify and retransmit so that the system of

and adding and subtracting from equation (4.5a) gives one

$$(3) \quad \frac{f}{(2-V)^2} = (1) \frac{f}{2^2} - \frac{1}{2(1)} = (2) \frac{f}{(2-V)^2} = \frac{1}{2} \Rightarrow \frac{f}{(2-V)^2} = \frac{1}{4}$$

$$(N_1, x) \pm d) \frac{1}{x^2} - \frac{1}{x^2} = (N_1, x) \pm d) \frac{1}{x^2}.$$

Assume that the time dependence will be of the form

$$\text{fol}_{\pi}^{-1}(x) \cap \pi^{-1}(a) = \text{fol}_{\pi}^{-1}(a) \cap \pi^{-1}(x) = (y, z) = d \pmod{2}$$

$$\langle \hat{x} \rangle = \frac{1}{\sqrt{2\pi}} \int_{-\infty}^{\infty} x e^{-\frac{x^2}{2}} dx = 0$$

removed (85%) from (a)–(d) avoiding bias.

$$u(x, y) = (x)^2 + (y)^2 + \frac{1}{x^2} + \frac{1}{y^2}$$

$$(1) \quad f(x) = a_0(x^2 + \frac{1}{x^2}) \quad (2) \quad f(x) = a_0(x^2 - \frac{1}{x^2})$$

where $k = \frac{\omega}{v+c}$

2. The Plate Equations

Again simplifying assumptions must be made. Neglecting the rigidity and the external forces on the plate, the normal mode form of the equations for this element can be derived in an analogous manner.

In putting the previous equations in simplified mode form, it is necessary to take linear combinations of the elemental forms. This is done by the following:

Let $\frac{\partial v(x,t)}{\partial x} \pm \frac{1}{\rho} \frac{\partial t}{\partial t} = \frac{\partial S(x,t)}{\partial t}$ where $v(x,t) = \frac{\partial \xi}{\partial t}$

where, the equations reduce to those needed for each element separately.

$$\frac{\partial v}{\partial t}(x,t) = \frac{\rho}{\rho} \frac{\partial S(x,t)}{\partial x} \quad S(x,t) = \frac{\partial \xi}{\partial x}$$

then

$$b_{\pm}(x,t) = \frac{1}{2} (\rho)^{\frac{1}{2}} (v(x,t) \pm \frac{\rho}{\rho} S(x,t))$$

and

$$\frac{\partial}{\partial x} (b_{\pm}(x,t)) = \mp (\frac{\rho}{\rho})^{\frac{1}{2}} \frac{\partial}{\partial t} (b_{\pm}(x,t))$$

therefore,

$$(\frac{\partial}{\partial x} - jk_2) a_{2+}(x) = 0 \quad (\frac{\partial}{\partial x} + jk_2) a_{2+}^* = 0 \quad (4.10a)$$

$$(\frac{\partial}{\partial x} + jk_2) a_{2-}(x) = 0 \quad (\frac{\partial}{\partial x} - jk_2) a_{2-}^* = 0 \quad (4.10b)$$

$$\text{where } \lambda = -\frac{2}{\alpha^2}$$

2. The Basic Equations

Again simplifying assumptions must be made. Inelastic flow the velocity and the normal stress on the plane, the normal mode form of the equations for this element can be derived in an analogous manner.

$$\frac{\partial v(x,t)}{\partial t} = \frac{\partial}{\partial x} \left(\frac{1}{\rho} \frac{\partial \sigma(x,t)}{\partial x} \right) \quad \text{where } \sigma(x,t) = \frac{1}{2} \rho v^2$$

$$\frac{\partial \sigma(x,t)}{\partial t} = \frac{\partial}{\partial x} \left(\frac{1}{\rho} \frac{\partial \sigma(x,t)}{\partial x} \right) \quad \text{where } \sigma(x,t) = \frac{1}{2} \rho v^2$$

then

$$\frac{\partial}{\partial t} \left(\frac{1}{2} \rho v^2 \right) = \frac{\partial}{\partial x} \left(\frac{1}{2} \rho v^2 \right)$$

and

$$\frac{\partial}{\partial t} \left(\frac{1}{2} \rho v^2 \right) = \frac{\partial}{\partial x} \left(\frac{1}{2} \rho v^2 \right)$$

therefore

$$(4.10a) \quad \left(\frac{1}{2} \rho v^2 \right) = \left(\frac{1}{2} \rho v^2 \right) + \left(\frac{1}{2} \rho v^2 \right) = 0$$

$$(4.10b) \quad \left(\frac{1}{2} \rho v^2 \right) = \left(\frac{1}{2} \rho v^2 \right) + \left(\frac{1}{2} \rho v^2 \right) = 0$$

where

$$k_2 = \frac{\omega}{(P/\rho)^{1/2}}$$

4.6 Coupling Between the Two Elements

In section B, we derived the normal mode form of the element equations. In effect the single variables in equations (4.8a) and (4.8b) have been replaced by a combination of the two variables. To put the previous equations in coupled mode form, it is necessary to make linear combinations of the elemental forms. This is done in such a manner that when the coupling is reduced to zero, the equations reduce to those derived for each element separately.

$$\frac{\partial a_1}{\partial x} = c_{11}a_1 + c_{12}a_2 + c_{13}a_1^* + c_{14}a_2^* \quad (4.11a)$$

$$\frac{\partial a_2}{\partial x} = c_{21}a_1 + c_{22}a_2 + c_{23}a_1^* + c_{24}a_2^* \quad (4.11b)$$

$$\frac{\partial a_1^*}{\partial x} = c_{31}a_1 + c_{32}a_2 + c_{33}a_1^* + c_{34}a_2^* \quad (4.11c)$$

$$\frac{\partial a_2^*}{\partial x} = c_{41}a_1 + c_{42}a_2 + c_{43}a_1^* + c_{44}a_2^* \quad (4.11d)$$

where

$$a_1 = \frac{1}{2} (\rho f)^{1/2} \sqrt{v_f(x)} + \frac{1}{\rho_0 (v+c)} \bar{p}(x)$$

$$\text{where } \frac{1}{\lambda^2} = \frac{1}{\lambda_1^2} + \frac{1}{\lambda_2^2}$$

1.6 Coupling between the elements

In section 5 we derived the normal mode form for the elementary equations. In effect the single variable in equations (5.1a) and (5.1b) have been replaced by a combination of the two variables. To put the previous equations in coupling mode form, it is necessary to make linear combinations of the elementary forms. This is done in such a manner that the coupling is reduced to zero, the equations reduce to those derived for each element separately

$$(6.1a) \quad \ddot{x}_1 + \omega_1^2 x_1 = \frac{1}{m} \left(F_1 \cos \omega t + F_2 \cos \omega t \right)$$

$$(6.1b) \quad \ddot{x}_2 + \omega_2^2 x_2 = \frac{1}{m} \left(F_2 \cos \omega t + F_1 \cos \omega t \right)$$

$$(6.1c) \quad \ddot{x}_1 + \omega_1^2 x_1 = \frac{1}{m} \left(F_1 \cos \omega t + F_2 \cos \omega t \right)$$

$$(6.1d) \quad \ddot{x}_2 + \omega_2^2 x_2 = \frac{1}{m} \left(F_2 \cos \omega t + F_1 \cos \omega t \right)$$

$$\text{where } \omega_1^2 = \frac{1}{m} \left(\frac{1}{\lambda_1^2} + \frac{1}{\lambda_2^2} \right) \quad \text{and} \quad \omega_2^2 = \frac{1}{m} \left(\frac{1}{\lambda_2^2} + \frac{1}{\lambda_1^2} \right)$$

$$a_2 = \frac{1}{2} (\rho_f)^{1/2} (\bar{V}_p(x) + \frac{\rho}{\rho_f} S(x))$$

and

$$c_{22} = -jk_2(1 + 1/4\rho_f k_2^2)$$

$$c_{32} = -j \frac{1}{4\rho_f k_2}$$

Δ coupling coefficient

In order to make the problem more tractable we must make use of our previous results. The first is that coupling between the two systems will occur when the two wave members, k_1 and k_2 , are approximately equal. Since $k_1 = \frac{\omega}{v-c}$ and $k_2 = \frac{\omega}{V_m}$ and in Chapter II we saw that the coupling occurred when $V_m + = V-c$, we can therefore neglect the fast fluid wave ($V+c$) and the backward plate wave (V_m-).

Secondly, we must determine if, in fact, the coupling between the two systems is weak. Returning to the coupled dispersion relationship and inserting our previous assumption that the rigidity and the magnetic field are zero, we have:

$$-(\bar{\omega}-\bar{k})^2 (\mu M_a^2 + M_m^2 k^2 - \bar{\omega}^2) + M_a^2 k^2 (-M_m^2 k^2 + \bar{\omega}^2) = 0$$

$$\frac{1}{\sqrt{1-x^2}} = 1 + \frac{1}{2}x^2 + \frac{3}{8}x^4 + \frac{5}{16}x^6 + \dots$$

our previous results. The first is that coupling between the two

systems will occur when the two wave numbers, k_1 and k_2 , are

approximately equal, then $\frac{m}{m+1} \approx \frac{m}{m+2}$ and $\frac{m}{m+1} \approx \frac{m}{m+3}$ only in cases of

we saw that the copying operation when $x = y = 0$, we can choose

Core neglect the last 700 years (see) and the modern place

1-2 V) 5V 5W

Secondly, we must determine if, in fact, the coupling between the two systems is weak. Referring to the coupled differential relationship and inserting our previous assumption that the electric and the magnetic field are zero, we have:

$$0 = \left(\frac{\partial}{\partial \omega} - \frac{1}{\omega} \right) \left(\frac{\partial}{\partial \omega} + \frac{1}{\omega} \right) \psi(\omega) = \left(\frac{\partial}{\partial \omega} - \frac{1}{\omega} \right)^2 \psi(\omega) \quad (\bar{\omega} = 0).$$

Therefore, eq. (4.11) and equation (4.10) reduce to
or in dimensional form and rearranged.

$$\{(\omega - V_0 k)^2 - c^2 k^2\} \{V_m^2 k^2 - \omega^2\} = \frac{\mu c^2}{d^2} (\omega - V_0 k)^2 \quad (4.12a)$$

where the term on the right represents the coupling between the two systems. Now let the perturbation of the elemental wave numbers be small:

$$k_1^* = \frac{\omega}{V-c} + \delta_1 \quad \text{where } \delta_1 \ll \frac{\omega}{V-c}$$

$$k_2^* = \frac{\omega}{V_m} + \delta_2 \quad \text{where } \delta_2 \ll \omega/V_m$$

and keeping second order terms in δ we find:

$$\delta_2(\delta_2 - \frac{V}{c} \delta_1) = - \frac{\mu c^3}{4d^2(V-c)^3}$$

If we now let $\delta_1 \rightarrow 0$ and recall that $v-c \approx c$, we see that:

1. The coupling is proportional to ratio of the densities of the two media μ , which is a small quantity, and

2. δ_2 is imaginary

$$\delta_2 = \pm j \left[\frac{\mu c^3}{4d^2(V-c)^3} \right]^{1/2}$$

and only if $V > c$

In the system under consideration

$$\frac{\omega}{V_m} = 1.00 \text{ ft}^{-1}$$

and

$$\delta_2 = 0.13 \text{ ft}^{-1}$$

or in dimensional form and rearranged:

$$\left\{ \left(\frac{a}{b} \right)^2 \left(\frac{b}{a} \right)^2 \right\} \left\{ \left(\frac{a}{b} \right)^2 \left(\frac{b}{a} \right)^2 \right\} \left\{ \left(\frac{a}{b} \right)^2 \left(\frac{b}{a} \right)^2 \right\} \left\{ \left(\frac{a}{b} \right)^2 \left(\frac{b}{a} \right)^2 \right\}$$

where the term in the right hand member the coupling between the two systems and the preservation of the dimensional wave numbers be small:

$$\frac{a}{b} \gg \frac{b}{a} \quad \text{where } \frac{a}{b} \gg \frac{b}{a}$$

$$\frac{a}{b} \gg \frac{b}{a} \quad \text{where } \frac{a}{b} \gg \frac{b}{a}$$

$$\frac{a}{b} \gg \frac{b}{a} \quad \text{where } \frac{a}{b} \gg \frac{b}{a}$$

If we now take $\frac{a}{b} \gg \frac{b}{a}$ and $\frac{a}{b} \gg \frac{b}{a}$, we see that:

The coupling is proportional to ratio of the lengths of the two media α , which is a small quantity, and

$$\frac{a}{b} \gg \frac{b}{a} \quad \text{where } \frac{a}{b} \gg \frac{b}{a}$$

In the system under consideration

$$\frac{a}{b} \gg \frac{b}{a} \quad \text{where } \frac{a}{b} \gg \frac{b}{a}$$

and

$$\frac{a}{b} \gg \frac{b}{a} \quad \text{where } \frac{a}{b} \gg \frac{b}{a}$$

Therefore, $c_{22} = jk_2$ and equations 4.11 reduce to:

$$\frac{\partial a_2}{\partial x} = -jk_2 a_2 + c_{23} a_1^* \quad (4.12a)$$

$$\frac{\partial a_1^*}{\partial x} = c_{32} a_2 + jk_1 a_1^* \quad (4.12b)$$

These equations can be solved by assuming solutions of the form $e^{\gamma x}$ and setting the determinant of the coefficients equal to zero.

$$\gamma_{1,2} = \pm \left[(c_{32})^2 - \frac{(k_1 - k_2)^2}{2} \right]^{\frac{1}{2}} j \left(\frac{k_1 + k_2}{2} \right) \quad (4.13)$$

where $k_1 = \frac{\omega}{V-c}$ and $k_2 = \frac{\omega}{V_m}$, the undisturbed elemental wave numbers.

Since they are approximately equal:

$$\gamma_{1,2} = \alpha - jk_2 \quad \text{where} \quad \alpha = (\delta_2) = \frac{\mu c^3}{4d^2(V-c)^2}$$

and the coupled modes can be represented as:

$$a_1^*(x) = A_1 e^{\delta_1 x} + A_2 e^{\delta_2 x}$$

$$a_2(x) = \left| \frac{1}{c_{32}} \right| \left((\delta_1 + jk_1) A_1 e^{\delta_1 x} + (\delta_2 + jk_1) A_2 e^{\delta_2 x} \right)$$

Therefore, $\psi_{\pm} = \psi_{\pm}^0 + \psi_{\pm}^1$ and equations (4.1) reduce to:

$$(4.12a) \quad \frac{\partial^2 \psi_{\pm}^0}{\partial x^2} + \frac{\partial^2 \psi_{\pm}^1}{\partial x^2} = -\frac{\partial^2 \psi_{\pm}^0}{\partial x^2} - \frac{\partial^2 \psi_{\pm}^1}{\partial x^2}$$

$$(4.12b) \quad \frac{\partial^2 \psi_{\pm}^0}{\partial x^2} + \frac{\partial^2 \psi_{\pm}^1}{\partial x^2} = -\frac{\partial^2 \psi_{\pm}^0}{\partial x^2} - \frac{\partial^2 \psi_{\pm}^1}{\partial x^2}$$

These equations can be solved by assuming solutions of the form $\psi_{\pm}^0 = A_{\pm} e^{ik_{\pm} x}$ and $\psi_{\pm}^1 = B_{\pm} e^{ik_{\pm} x}$. The boundary conditions are:

or

$$(4.13) \quad \psi_{\pm}^0 = A_{\pm} e^{ik_{\pm} x} + B_{\pm} e^{-ik_{\pm} x} + \frac{1}{2} \left[\frac{(k_{\pm}^2 - \frac{1}{2})}{k_{\pm}} e^{ik_{\pm} x} + \frac{(k_{\pm}^2 - \frac{1}{2})}{k_{\pm}} e^{-ik_{\pm} x} \right]$$

where $k_{\pm} = \frac{10}{\sqrt{2}}$ and $k_{\pm}^2 = \frac{1}{2}$. The unperturbed classical wave number is:

Since they are exponentially small:

$$(4.14) \quad \frac{\partial^2 \psi_{\pm}^0}{\partial x^2} + \frac{\partial^2 \psi_{\pm}^1}{\partial x^2} = -\frac{\partial^2 \psi_{\pm}^0}{\partial x^2} - \frac{\partial^2 \psi_{\pm}^1}{\partial x^2} \quad \text{where} \quad \frac{\partial^2 \psi_{\pm}^0}{\partial x^2} = -\frac{\partial^2 \psi_{\pm}^1}{\partial x^2}$$

and the perturbed wave can be represented as:

$$\psi_{\pm}^1(x) = A_{\pm} e^{ik_{\pm} x} + B_{\pm} e^{-ik_{\pm} x}$$

$$\psi_{\pm}^1(x) = A_{\pm} e^{ik_{\pm} x} + B_{\pm} e^{-ik_{\pm} x} + \frac{1}{2} \left[\frac{(k_{\pm}^2 - \frac{1}{2})}{k_{\pm}} e^{ik_{\pm} x} + \frac{(k_{\pm}^2 - \frac{1}{2})}{k_{\pm}} e^{-ik_{\pm} x} \right]$$

4.7 Summary

The eigenvalue problem has been stated, but was not solved because the method of coupling of modes gave better insight into this problem. We applied coupling of modes to a simplified problem and determined the perturbation of the wave numbers based on the effect of the coupling. In order to properly apply the boundary conditions in this case, the approach of coupling of modes could be followed. But it is not clear that the neglected waves can in fact, be neglected. Since at long wave lengths, the boundaries will have a definite effect on both modes, this must be accounted for in the theory. The results of Chapter III and IV do provide a basis for experimentation. If we assume that the wave numbers are only slightly perturbed; we can compute k_r from the physical length, k_i from equation 4.13 and ω_r and ω_i from the dispersion relationship. Although these values are not exactly self-consistent, they should be approximately so. The Experimental techniques to achieve these values are described in the next section.

The next section is devoted to the experimental techniques. Due to the difficulty of the experiment, the results of this test were qualitative rather than quantitative. The results are shown in table 4.1. The end conditions have a noticeable effect on the response. The frequency is slightly higher than that slightly higher than the theoretical value.

The frequency and amplitude were measured which indicates that the use of the coupling of modes in the coupling of modes is not invalid in error. The frequency is slightly higher than the theoretical value.

The eigenvalue problem has been stated, but was not solved because the method of coupling of modes gave better insight into this problem. The coupled coupling of modes in a simplified problem and determined the structure of the wave number space in the limit of the coupling. In order to proceed to study the boundary conditions in this case, the approach of coupling of modes could be followed. It is to be clear that the coupling waves can in fact, be neglected. Since at long wave lengths, the boundary will have a definite effect on both modes, this must be accounted for in the theory. The results of Chapter IV and IV do provide a basis for investigation. It is shown that the wave number are still slightly perturbed, as can be seen from the physical length. The coupling of modes is not from the dispersion relations. Although these values are not exactly self-consistent, they should be approximately so. Experimental techniques to achieve these values are indicated in the next section.

CHAPTER V

EXPERIMENTAL PROCEDURE

In order to experimentally test the predictions of the theory developed, it is necessary first to insure that the "ingredients" required are available. The initial attempt at assembling a device and making test runs was not successful. The step by step approach will be described in detail. This consisted of several separate experiments. The first was testing of the plate structure to be used. The second was investigation of a means of attaining supersonic flow. Next, the two were combined to test the flutter theory.

5.1 Testing of the Plate

There were two experiments performed on the plate along. The first was an investigation of various types of material and various end conditions. The test set up is shown schematically in Figure 5.1. Due to the magnetic coupling between the two circuits, the results of this test were qualitative rather than quantitative. The results are shown in table 5.1. The end conditions have a noticeable effect on the response. The damping or losses in ^{any} condition but tightly clamped appeared to nullify any response.

The frequency did increase with tension which indicates that the use of membrane analysis in the coupling of modes section is not totally in error. The frequency of response was reasonably

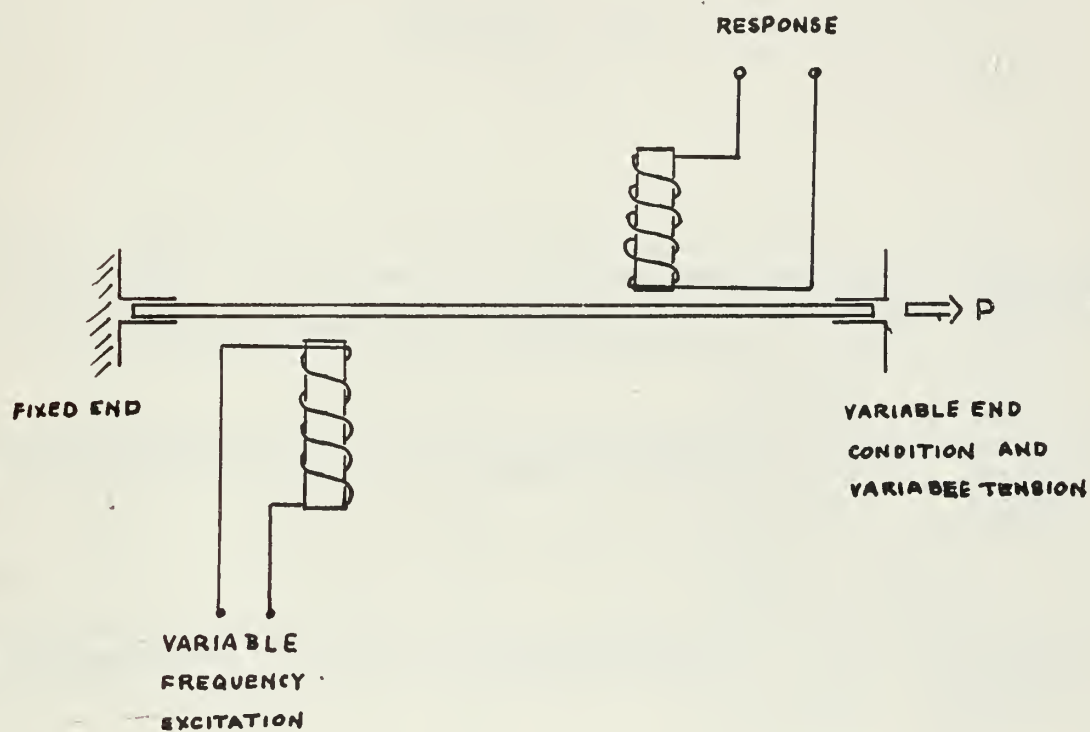
1.1.1. Introduction

In order to experimentally test the predictions of the theory developed, it is necessary first to know that the "instabilities" required are available. The initial design of assembling a device and making test runs was not successful. The step by step approach will be described in detail. This consisted of several separate experiments. The first was testing of the plate structure to be used. The second was investigation of a means of achieving synchronous flow. Next, the two were joined to test the linear theory.

1.1.2. Testing of the Plate

There were two experiments performed on the plate alone. The first was an investigation of various modes of natural and forced vibration and conditions. However, it was shown experimentally in Figure 1.1 that the results of the two experiments were not additive. The results are shown in Table 1.1. The conditions have a noticeable effect on the response. For example, the results for linear and nonlinear analysis are not additive. The results are shown in Table 1.1. The results are shown in Table 1.1. The results are shown in Table 1.1.

The frequency of the response with respect to which the results are shown in Table 1.1. The frequency of the response is not additive in respect. The frequency of the response is not additive in respect.



TOP VIEW OF TEST SECTION

FIGURE 5.1

TABLE 5.1

SAMPLE	DIMENSIONS	END CONDITIONS	FREQUENCY	RESPONSE
1 COLD ROLLED IRON	6x1x.030 (inches)	CLAMPED-CLAMPED	51 (CPS) 103 300	SMALL SMALL SMALL
2 HEAT TREATED STEEL	8x1x.015	CLAMPED-CLAMPED	63 112	LARGE MEDIUM
3 SPRING STEEL	6x1x.015	CLAMPED-CLAMPED	70 140	MEDIUM SMALL
SAMPLE 2		CLAMPED-PINNED NO TENSION	—	NONE
SAMPLE 2		CLAMPED-PINNED TENSION	75 148	LARGE MEDIUM

close to that predicted. (See example 5.1)

EXAMPLE 5-1
$$\omega_m^2 = \pi^2 \frac{m^2}{l^2} + \frac{n^2}{w^2} \frac{P}{\mu}$$

where

$D = EI$, the rigidity

μ = mass per unit area

M = longitudinal harmonic mode

l = length

$$\omega_2 = 650 \frac{1}{\text{sec}}$$

$$f_2 = 104 \text{ cps}$$

The second experiment on the plate above was to determine if in fact the second harmonic frequency could be excited when the media had the predominate properties of a membrane. Equipment similar to that shown in Figure 5.1, was used for this part of the experimentation. To avoid the magnetic coupling, one of the electromagnets was replaced by a speaker for mechanical excitation with weak coupling. The plate thickness was reduced to .001 inch, to more closely approximate a membrane. The equipment is shown pictorially in Figure 5.

In this configuration the plate frequencies were not detectable. The membrane frequencies gave excellent response and are tabulated in Table 5.3. The variation between predicted and

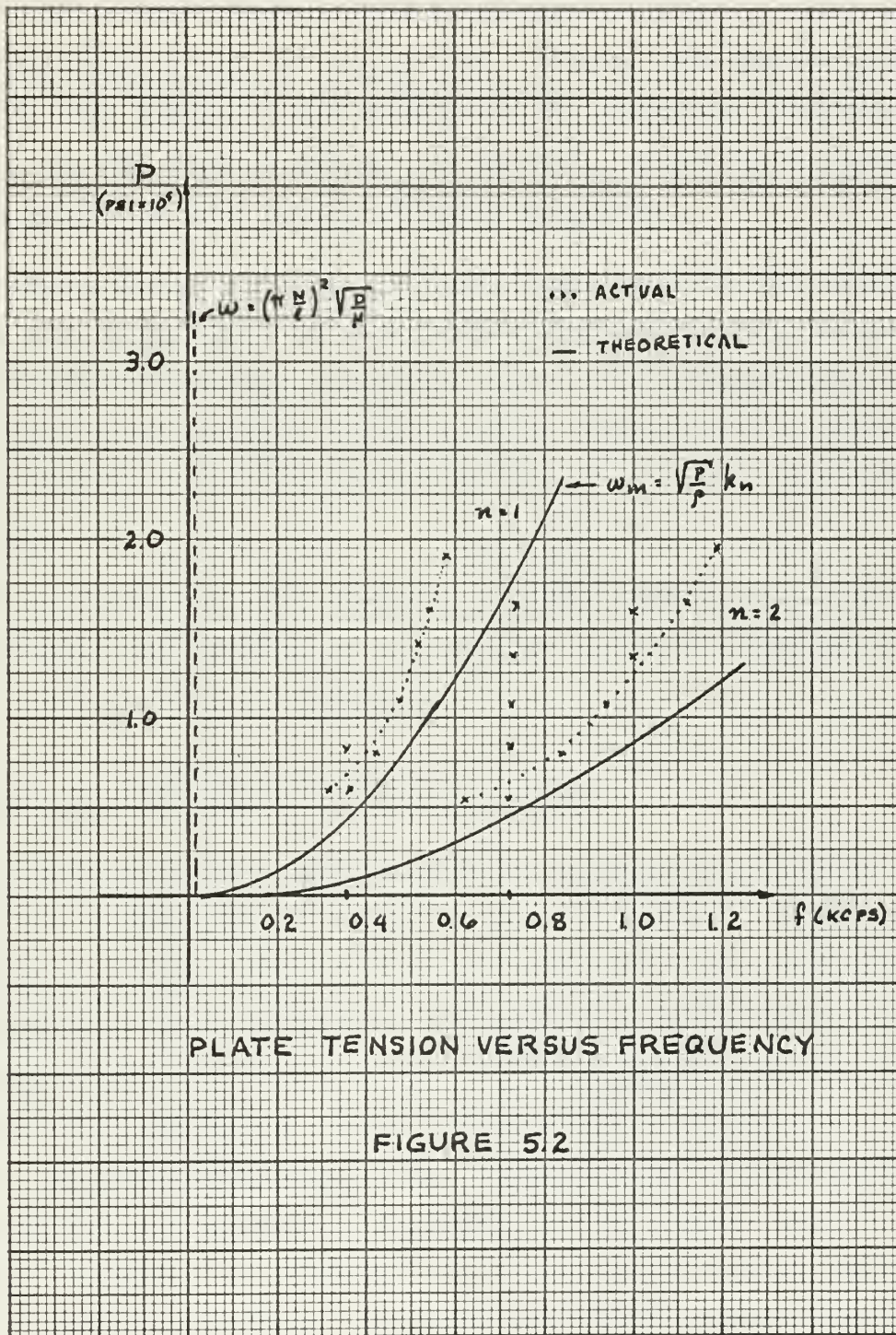
close to that predicted. (See example 2.1.)

$$\text{EXAMPLE 2.1} \quad \omega_1 = \sqrt{\frac{E}{\rho}} \sqrt{\frac{1}{L^3}} \quad \omega_2 = \sqrt{\frac{E}{\rho}} \sqrt{\frac{4}{L^3}} \quad \omega_3 = \sqrt{\frac{E}{\rho}} \sqrt{\frac{9}{L^3}}$$

where $E = 31$, the rigidity
 $\rho = 2.5$ g/cm³
 $L = 10$ longitudinal harmonic units
 $L = 10$ length
 $\omega_1 = 650$ rad/sec
 $\omega_2 = 104$ cps

The second experiment on the plate shows that in fact the second harmonic frequency could be excited when the media had the harmonic properties of a harmonic oscillator. It is similar to that shown in Figure 2.1, was used for this part of the experiment. To make the harmonic coupling, one of the electrostatics was replaced by a speaker for mechanical excitation with weak coupling. The plate thickness was reduced to 1.01 inch, to more closely approximate a harmonic oscillator. The experiment is shown pictorially in Figure 2.

In this configuration the plate transducer gave an excellent cable. The harmonic frequencies were excellent frequency and were calculated in Table 2.2. The variation between predicted and



actual frequencies can be explained. First, the actual parameters for the material are difficult to determine exactly. Secondly, at the higher values of tension, there is a possibility that the grips or end clamps slipped slightly.

The main conclusion to be drawn here is that the second harmonic can definitely be observed. The quality of the response decrease with increasing frequency since the higher modes are more difficult to exert. The frequency expected when operating the wind tunnel could be reasonably predicted from this type of experiment

The responses at 355 and 720 cps are probably due to weak coupling with the speaker or other portion of the apparatus, since they are independent of tension.

5.2 Experiment to Obtain Supersonic Flow.

The physics of supersonic flow is a very complicated subject and is extensively covered in the literature, notably in reference 15. Only those principles which are germane to this experiment will be touched on. In general, supersonic flow can not be attained directly from an air compressor. It is necessary to modify the compressor output by passing it through a set of nozzles. For this experiment the nozzles were of the convergent-divergent type. The design procedure is to attain Mach 1 flow at the throat of the test section and then expand to the velocity desired. The calculations for this are shown in example 5.2,

actual frequencies can be explained. First, the actual frequencies for the material are difficult to determine exactly. Secondly, at the higher values of tension, there is a possibility that the edges of end clamps slipped slightly.

The main conclusion to be drawn here is that the second harmonic can definitely be observed. The quality of the resonance decreases with increasing frequency along the higher modes are more difficult to excite. The frequency measured when operating the wind tunnel could be reasonably predicted from this type of experiment.

The responses at 155 and 170 cps are probably due to modes coupling with the speaker or other portion of the apparatus, since they are independent of tension.

5.2 Experiment to Obtain Unsteady Flow

The physics of supersonic flow is a very complicated subject and is extensively covered in the literature, notably in reference 12. Only those principles which are known to this experiment will be covered on. In general, supersonic flow can not be excited directly from an air compressor. It is necessary to modify the compressor output by passing it through a set of nozzles. In this experiment the nozzles were of the convergent-divergent type. The design procedure is to obtain such a flow at the throat of the test section and then expand to the velocity desired. The calculations for this are shown in appendix 5.1.

based on the set of nozzles shown in Figure 5.4.

EXAMPLE 5.2 (Reference 15, Table BIII)

Inlet Conditions:

$$P_o = 125 \text{ psia} \quad T_o = 70^\circ\text{F}$$

a. Static Conditions:

$$\rho_o = \frac{P_o}{RT_o} = 0.605 \frac{\text{m}}{\text{ft}^3}$$

$$c_o = 49.1 \quad T_o = 1158 \frac{\text{ft.}}{\text{sec.}}$$

b. Throat Conditions:

$$P^*/P_o = 0.528$$

$$T^*/T_o = 0.823$$

$$\rho^*/\rho_o = 0.634$$

$$c^*/c_o = 0.913$$

c Test section conditions for Mach No. = 2.0

$$M^* = 1.633$$

$$A/A^* = 1.687$$

$$A_{\text{test}} = 6.0 \text{ cm}^2$$

$$P_1/P_o = 0.1278$$

$$V = 1733 \text{ ft/sec}$$

$$A_{\text{throat}} = 3.57 \text{ cm}^2$$

$$\rho_1/\rho_o = 0.2300$$

$$P_1 = 16.1 \text{ psia}$$

$$T_1/T_o = 0.555$$

d. Mass Flow

$$A^* \times 60 = 245 \text{ cuft/min.}$$

based on the set of numbers shown in Figure 1.

Figure 1. The numbers 1 through 10.

Figure 1. The numbers 1 through 10.

Figure 1. The numbers 1 through 10.

Figure 1. The numbers 1 through 10.

Figure 1. The numbers 1 through 10.

Figure 1. The numbers 1 through 10.

Figure 1. The numbers 1 through 10.

Figure 1. The numbers 1 through 10.

Figure 1. The numbers 1 through 10.

Figure 1. The numbers 1 through 10.

Figure 1. The numbers 1 through 10.

Figure 1. The numbers 1 through 10.

Figure 1. The numbers 1 through 10.

Figure 1. The numbers 1 through 10.

Figure 1. The numbers 1 through 10.

Figure 1. The numbers 1 through 10.

Figure 1. The numbers 1 through 10.

Figure 1. The numbers 1 through 10.

Figure 1. The numbers 1 through 10.

Figure 1. The numbers 1 through 10.

Figure 1. The numbers 1 through 10.

Figure 1. The numbers 1 through 10.

Figure 1. The numbers 1 through 10.

Figure 1. The numbers 1 through 10.

Figure 1. The numbers 1 through 10.

Figure 1. The numbers 1 through 10.

Figure 1. The numbers 1 through 10.

Figure 1. The numbers 1 through 10.

Figure 1. The numbers 1 through 10.

Figure 1. The numbers 1 through 10.

Figure 1. The numbers 1 through 10.

Figure 1. The numbers 1 through 10.

Figure 1. The numbers 1 through 10.

Figure 1. The numbers 1 through 10.

Figure 1. The numbers 1 through 10.

Figure 1. The numbers 1 through 10.

Secondly, the flow in the test section will be greatly effected by the build up of the boundary layer. This has the effect of a convergent nozzle, which tends to reduce to flow velocity toward Mach 1. In the case of Mach 2 flow, the velocity will be reduced to Mach 1 in a length of 31 diameters. In this experiment, the diameter or depth of the channel will be taken as one centimeter to allow sufficient magnetic coupling. Therefore, the length must be less than 31 centimeters; an initial length of 20 centimeters was used. (From this length, the thickness of the plate for a desired natural frequency can be computed as in example 5.1). Based on these calculations, the experiment shown schematically in Figure 5.3 and was constructed.

The pressure readings were taken with both the plate in position and removed. The readings were taken with a guage and compared with a monometer for accuracy. The readings obtained are shown in Figure 5.4.

These results are at a variance with those predicted in example 5.2, but they do indicate supersonic flow. The variance is due to several factors. First, the ideal area ratios are significantly diminished by the boundary layer to an "effective" area ratio. Secondly, the capacity of the air ejectors was insufficient for running the experiment as desired. Also, the pressure measurements were made at the wall of the channel, probably in the boundary layer, and not in the center of the flow. The latter problem is difficult to circumvent, and in previous experiments (reference 15, page 135) good agreement between actual

FIGURE 5.3

Secondly, the flow in the case section will be greatly affected by the build up of the boundary layer. This has the effect of a convergent nozzle, which tends to reduce the flow velocity toward each end. In the case of such a flow, the velocity will be reduced to half in a length of 11 diameters. In this experiment, the diameter or length of the channel will be taken as one diameter to give sufficient margin for safety. Therefore, the length must be less than 11 diameters as this end length of 10 diameters was used. (Upon this length, the thickness of the plate has a desired natural frequency can be computed as in example 2.1). Based on these relations, the experiment shown schematically in Figure 2.3 was conducted.

The pressure readings were taken with both the plate in position and removed. The readings were taken with a gauge and compared with a manometer for accuracy. The readings obtained are shown in Figure 2.4.

These results are at a variance with those predicted in example 2.1. The flow is highly viscous. The distance is too close to the boundary layer. First, the ideal area ratio is slightly diminished by the boundary layer to an "effective" area ratio. Secondly, the capacity of the air column was investigated for running the experiment as desired. Also, the pressure measurements were made at the wall of the channel, not only in the boundary layer, but also in the center of the flow. The latter problem is difficult to circumvent, and in previous experiments (reference 1, page 11) good agreement between actual

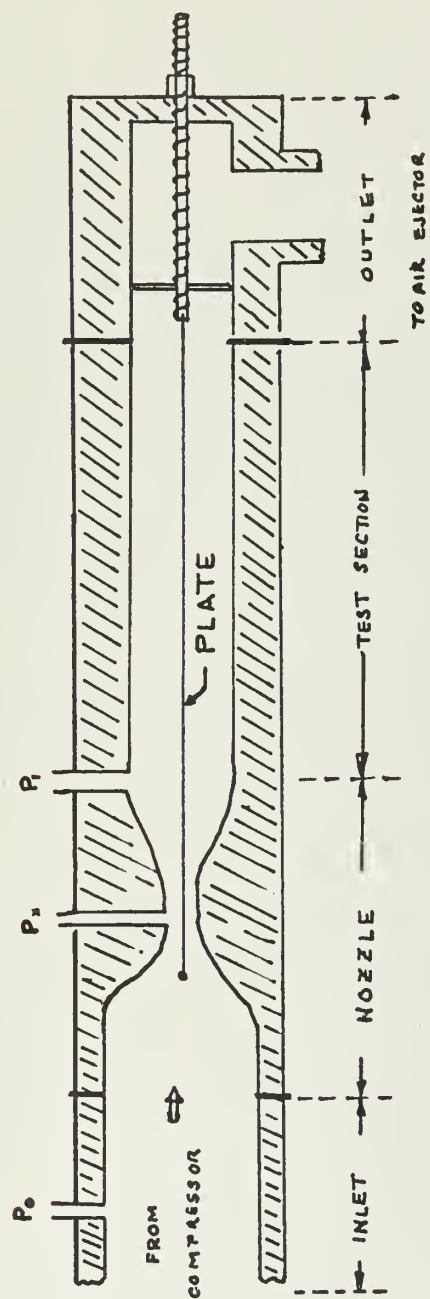
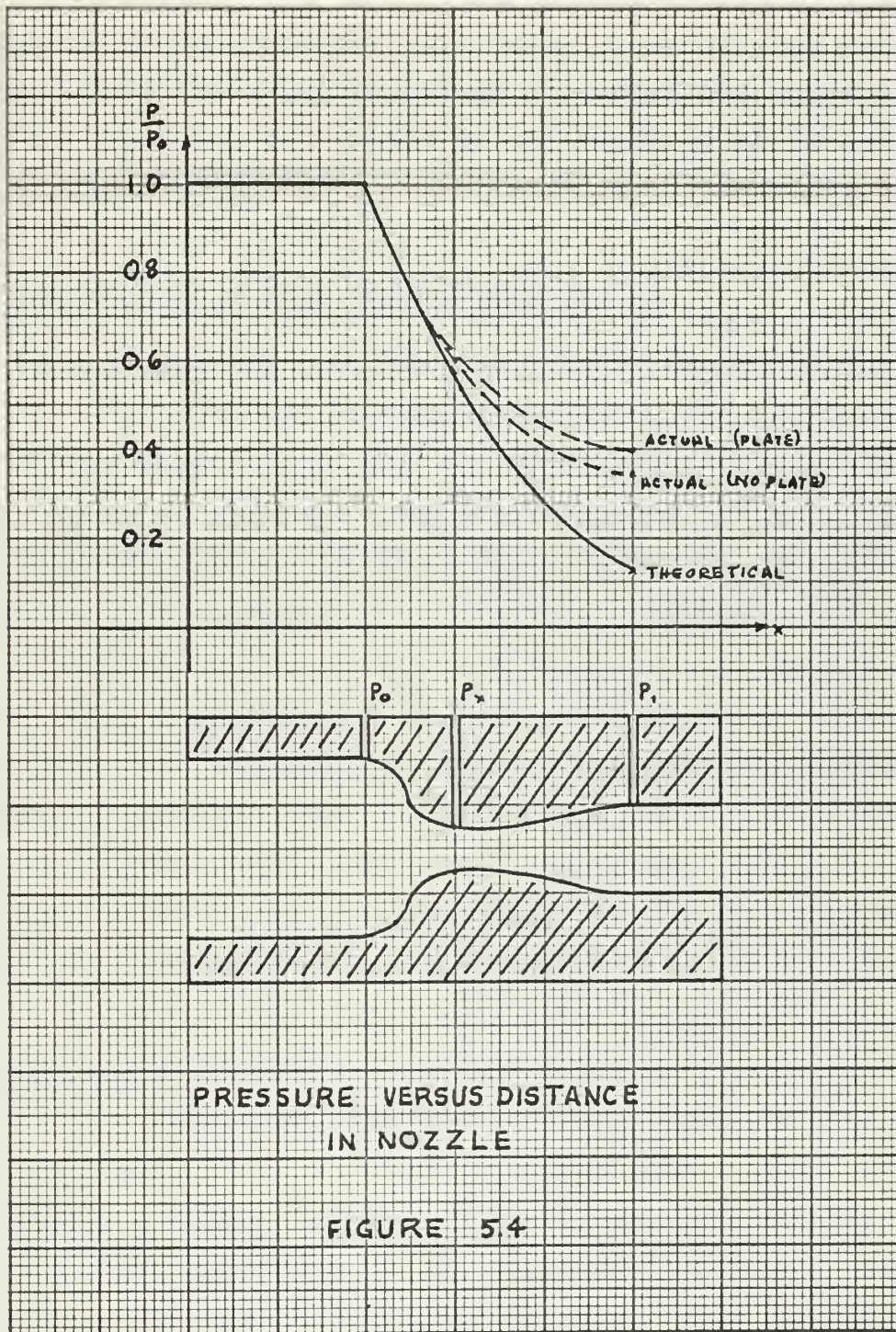


FIGURE 5.3

NOZZLE TEST SECTION



wall pressure and theoretical mid-stream pressures has been attained. Using the lower pressures recorded, the speed of the flow can be approximated. Based on the readings at 35 psia inlet, the flow is Mach 1.47.

5.3 An Experiment to Test the Flutter Theory

We have determined that the ingredients of the theory are attainable. The flow can be made supersonic, the plate can be excited in the second mode, and the frequency of this mode varies with the tension. Thus the results of Chapter IV indicating that the perturbation on the wave number k can be estimated from the coupling seem reasonable. The rigidity term Dk^2 can be neglected compared to the membrane term M_m^2 at the frequencies in question. This is especially true if the very thin (.001") plate is used. The first experiments with the combined ingredients used a .015 inch plate. The equipment consisted of the nozzle, a plate, a magnetic detection device and an oscilloscope. The presentation on the scope was confused, showing standing waves and traveling waves and these responses were at several frequencies. These were probably excited by the boundary layer. The tension was varied and the frequencies of the response increased with increasing tension. By varying the pressure the response would set in at a certain pressure for a given tension - quantitatively a higher tension required a higher pressure. At a given pressure, providing it was above the threshold, the varying of the tension was limited mechanically. That is, the tension

all pressure and theoretical differences between the two
 occurred. Using the limit pressure recorded, the value of the
 flow can be approximated. Based on the condition at 27 psi inlet,
 the flow is about 1.47.

3.1 An Experiment to Test the Limit Theory

We have determined that the limit theory of the theory can
 be verified. The flow can be approximated, the limit can be
 reached in the second order, and the pressure of this limit
 step the condition. From the results of Chapter IV indicated
 that the perturbation of the flow cannot be reached from
 the working area condition. The stability test can be
 neglected compared to the condition test M^2 at the transition to
 question. This is especially true in the very high (1.00) plate
 is used. The first experiment with the combined instrument
 used a 0.5 inch plate. The experiment consisted of the nozzle,
 a plate, a magnetic induction device and an accelerometer. The
 presentation on the theory was indicated, showing standing waves
 and traveling waves and their responses were at constant fre-
 quencies. These were specially varied by the boundary layer.
 The condition was varied and the responses of the response
 increased with increasing condition. By varying the pressure the
 response would not be a certain pressure for a given condition -
 potentially a higher condition required a higher pressure. At
 a given pressure, however, it was shown the threshold, the very-
 ing of the condition was independent of the condition. That is, the condition

could be increased until the plate failed in tension, and if the tension was decreased the plate would fail by excessive displacement. The latter occurred at low values of tension. It was felt that nothing of substance to support the theory could be gained from further experimentation with this set up. "Flutter" did occur and this did provide a variable coupling between the two magnetic circuits and there was an output signal.

However, this flutter could not be attributed exclusively to the mechanism proposed in the theory. It was probably caused by excitation from the boundary layer. There was a component in the vicinity of the frequency expected as computed below:

$$(1) \text{ length of membrane: } k = \frac{2\pi}{L} = .628 \text{ in}^{-1}$$

$$(2) \text{ from dispersion equation: } f = \frac{(M_a - 1)kv_o}{2\pi} = 1080 \text{ cps}$$

$$\omega_i = 495 \text{ sec}^{-1}$$

$$(3) \text{ from coupling of modes: } \alpha = \frac{\mu c^3}{4d^2(v-c)^2} = .25 \text{ in}^{-1}$$

In order to prevent the end connection from interfering with the flow they were removed from the test section as shown in the figure. Therefore, the flow is in transition over a short

could be maintained until the plane failed to contain, and in the
 reaction was observed that this could still be maintained in-
 glycerine. The latter occurred at low rates of reaction. It was
 this rate involving of substances to support the theory could be
 gained from further experimentation with this set up. "Fluoride"
 did occur and this did provide a variable coupling between the
 two magnetic circuits and there was no other effect.

However, this theory could not be maintained consistently
 in the mechanism proposed in the theory. It was previously assumed
 by calculation from the boundary layer, that was a component in
 the vicinity of the frequency required as indicated below:

$$(1) \text{ Length of element: } L = \frac{2\pi}{\omega} = 2.0 \times 10^{-1} \text{ m}$$

$$(2) \text{ Inductance element: } L = \frac{\mu_0 \mu_r N^2 A}{2\pi} = 1.0 \times 10^{-1} \text{ H}$$

$$R = 1.0 \times 10^{-1} \text{ ohm}$$

$$(3) \text{ From equation (1) above: } \omega = \frac{2\pi}{L} = 1.0 \times 10^1 \text{ rad/sec}$$

In order to observe this and determine from interesting
 data the theory may be tested from the data section as shown
 in the figure. Therefore, the theory is in agreement with a short

section at both ends of the plate. This could also provide an excitation which was not predicted and would be difficult to analyze.

Therefore, another experiment was designed. Due to a time problem, it may not be completed before the due date of this thesis. The changes include using a .001 inch plate to more closely approximate membrane performance, refined end connectors to insure a good response and no flow disturbance by the tension mechanism. The results of this phase of the experimentation will be reported in Appendix B.

section at both ends of the block. This case also occurs as
 condition which was not predicted and would be difficult to
 analyze.

Therefore, another experiment was devised. It is a two
 phase, it may not be completed before the date of this
 issue. The object was to raise a 100 lb. plate to some
 easily accessible position, and then disassemble it by the system
 to prove a good system and as the disassembly by the system
 mechanism. The results of this phase of the investigation will
 be reported in a separate report.

CHAPTER VI

CONCLUSIONS AND RECOMMENDATIONS6.1 Conclusions

The analysis of the model does predict the desired phenomenon. The interaction between the flow and the elastic media at long wavelengths will theoretically produce growing oscillations. The effects of the longitudinal boundary conditions can be approached by the coupling of modes. In the simplified problem considered in Chapter IV, the effect of the coupling on the wave number was shown. This approach could be expanded to show the influence of the boundaries on the wave numbers.

The experimental portion shows that the separate systems can be achieved. The plate can be excited in the second mode. The natural frequencies of the plate increase with tension and the tension required by the theory is physically realizable. A supersonic flow over the plate can also be attained in the laboratory. With the equipment used, the maximum velocity was 1.47 times the speed of sound. The major source of difficulty encountered in combining the systems was the excitation provided by the boundary layer. This was not included in the model or in the analysis. The excitation gave forced responses, mainly in the first mode, although there was a second mode in the response.

There are several other considerations which have not been covered. With respect to the elastic media, there will be eddy currents induced when it oscillates in the magnetic field.

CHAPTER IV

CONCLUSIONS AND DISCUSSION4.1 Conclusions

The analysis of the model has revealed the following conclusions. The interaction between the film and the elastic media at long wavelengths will characteristically produce resonant behavior. The effects of the longitudinal boundary conditions can be approximated by the coupling of modes. In the present case, this is considered in Chapter IV, the effect of the coupling on the wave number was shown. This approach would be extended to show the influence of the boundaries on the wave number.

The experimental portion shows that the acoustic system can be realized. The plate can be excited in the desired mode. The natural frequencies of the plate increase with tension and the tension required by the theory is physically reasonable. A comparison of the theory with the data can also be obtained in the future.

With the equipment used, the wave number was 1.4 times the speed of sound. The major source of difficulty encountered in conducting the system was the excitation provided by the boundary layer. This was not included in the model as in the analysis. The excitation gave forced responses, mainly in the first mode, although there was a second mode in the response.

There are several other considerations which have not been covered. With tension in the elastic media, there will be a constant induced stress in the magnetic field.

These represent a loss in the system which could be significant. The Curie temperature will impose a thermal limitation, restricting efficient operation of the device to relatively low temperatures. From the stand point of strength, it is fortunate that ferrous materials, which are required magnetically, also show good fatigue properties.

The most severe limitation on the device efficiency will be the losses incurred by the fluid in transiting the nozzle and interaction area. It was noted in the experimental section that the flow would be supersonic only for a short distance. For instance, the Mach 1.47 flow in the experiment would be "choked" to Mach 1.0 at the end of the test section (six inches), due to boundary layer build up. At the same time the isentropic stagnation pressure would be reduced to less than one half its initial values. This represents a considerable loss in efficiency. A more refined design would improve on this situation, but there will be a definite limiting efficiency attainable.

The subject of supersonic flow in short ducts is somewhat complex and experimental data has not been consistent. (15)

In general, the boundary layer thickness increases with length. But in some cases, negative friction coefficients have been attained, indicating a decreasing boundary layer. The effects of the oscillating plate on the boundary layer have also been studied but there appears to be no significant change in boundary layer thickness. (16)

These two views are found in the same area and are identical. The other two views are found in the same area and are identical. The other two views are found in the same area and are identical.

The most severe limitation on the device efficiency will be the losses incurred by the fluid in its passage through the device. It was noted in the experimental section that the flow would be approximately half that of a single stage. In addition, the head loss in the experimental device was about 1.0 at the end of the test section (see Figure 1). At the same time the laminar flow boundary layer built up. At the same time the laminar flow boundary layer built up. At the same time the laminar flow boundary layer built up.

The subject of *transmission* (the in short time to transfer
copies and experimental data was not very constant)
(11)

In general, the boundary layer thickness increases with length
but in some cases, massive injection oscillations have been
attained, indicating a decreasing boundary layer. The effects
of the oscillation phase on the boundary layer have also been
studied and these aspects to be in significant change in boundary
layer thickness. (12)

The device itself may not be the most efficient way of obtaining energy from the flow. However, it is possible that to employ it in tandem with a ~~more~~ conventional energy converter would improve overall efficiency. The important conclusion here is that a mechanism is available for transfer of energy between the flow and the media. The mechanism itself is not a "lossy" one - the inefficiencies are incurred in the scheme for using the mechanism attempted here. In other words, this paper has been limited in scope to a particular device, but further research would lead to other methods of using this concept for energy transfer.

6.2 Recommendations

The study of the longitudinal boundary conditions in this scheme could be expanded using the coupling of modes approach. The coupling coefficients considered here pertained only to the coupling between two waves, one in each system. The coupling between the other two waves, both with the other wave in its own system and the other wave in the other system were neglected. The latter still appears reasonable. But the boundary conditions will provide coupling between the two waves in one system. We neglected this here because at the wavelengths in question, the rigidity term could be neglected and the plate considered as a membrane. In the general case this would not be so, and the area of longitudinal boundary conditions in coupled systems has many possibilities for study.

The device itself may not be the most efficient way of obtaining energy from the free energy, it is possible that an engine is in the future. This is a very important point. The second point is that a mechanism is available for conversion of energy between the two and the other. The mechanism itself is not a "loss" one - the limitations are limited in the future. For using the mechanism according to the other point, this paper has been limited in scope to a preliminary design, but further research will lead to other methods of using this energy for energy transfer.

The study of the linguistic boundary conditions in this
system could be expanded using the coupling of water resources.
The coupling conditions considered here represent only a
coupling between two rivers, not in any system. The coupling
between the other two rivers, both with the other river in the
system and the other river in the other system were neglected.
The latter will require research. The boundary conditions
will provide similar results for the other two rivers. The
neglected river here however as the boundary is constant, the
system will be neglected and the other considered as a
boundary. In the present case this would not be so, and the
of linguistic boundary conditions in a coupled system has been
considered for the study.

The combined experiment showed the over-~~com~~standing effect of the boundary layer, essentially masking the desired response if present. The boundary layer could be reduced either by thermal methods or by expanding the flow in the depth dimension. If this were done, the correlation of experiment and theory might be attained and the mechanism studied.

Ketterer⁽⁹⁾ used a fluid stream and a spring coupled electrically to study this mechanism. Fraize⁽¹⁷⁾ studied a device in which a fin, situated in a wind tunnel (sub sonic), was excited mechanically to produce traveling waves. Significant reductions in drag were recorded. Replacing the mechanical excitation by magnetic traction along the length, using the coupling mechanism investigated here, provides the possibility for pumping of or propulsion through a fluid surrounding the fin

This would be the inverse of the problem studied here, but would not have the boundary layer problem inherent in super sonic flow.

The combined experiment shows the quantitative relationship
and primary layer, especially within the basal portion
of the layer. The primary layer could be regarded as
formed, without or by separating the film in the basal direction.
It is also seen, the separation of specimens and layer
might be attained and the specimen retained.

Figure 1 shows a cross-section and a series of
micrographs to show this relationship. Figure 1 shows a
layer is shown in a cross-section (Fig. 1a) and
and excited optically to produce a series of
and radiation to form more complex. The radiation
excitation by visible radiation along the layer, using the
long wavelength infrared light, provides the possibility of
probing at or monitoring through a thin specimen and the
This would be the image of the polymer studied here and
would not have the boundary layer problem inherent in other
ionic flow.

Appendix A

A COMPARISON WITH FLUTTER THEORY

Flutter is defined as the self-excited oscillations of a airfoil in supersonic flow.⁽¹⁸⁾ This definition leaves some doubt as to the physics involved, but since it is restricted to supersonic flow it seems conceivable that the mechanism involved is similar to the feedback situation described in Chapter III.

The problem of flutter is stated as a partial differential equation, where structural, inertial, and also dynamic operators are combined to determine the equation of motion for the panel. Two approaches are followed from here depending on the geometry involved. One is to apply the boundary conditions to the plate only. Since these are two at each end, a "fourth order" eigenvalue problem results.

The second approach is to assume traveling wave solutions, $e^{jkx-\omega t}$, and assuming real values for k , compute complex values of ω . Dugandji⁽¹⁹⁾ has used both approaches and compared the results. He then recommends which approach to use based on the geometry of the problem considered.

In terms of our parameters, the equation of motion is:

$$D \frac{\partial^4 \xi}{\partial x^4} - P \frac{\partial^2 \xi}{\partial x^2} + 2\rho\Delta \frac{\partial^2 \xi}{\partial t^2} + G_s \frac{\partial \xi}{\partial t}$$

$$= \frac{\rho c^2 v_o}{(1-M_a^2)^{1/2}} \left(\frac{\partial \xi}{\partial x} + \left(\frac{1-2M_a^2}{1-M_a^2} \right) \frac{1}{v_o} \frac{\partial \xi}{\partial t} \right)$$

where the term on the right is the "aerodynamic pressure." For small M_a , this reduces to

$$= \rho c^2 \left(\frac{\partial \xi}{\partial t} + v_o \frac{\partial \xi}{\partial x} \right)$$

and the equation is the same as equation (2.10) except for the structural damping term G_s . In our case, the aspect ratio is zero and the first approach is recommended. That is: the boundary conditions on the plate are applied and a solution of the form

$$\xi = (\xi_1 e^{k_1 x} + \xi_2 e^{k_2 x} + \xi_3 e^{k_3 x} + \xi_4 e^{k_4 x}) e^{j\omega t}$$

is assumed. This forms the eigenvalue problem, and the solutions for ω_r , ω_i are shown in reference 18. Many parameters have been introduced and this leads to lengthy computations to compare the

$$\sum_{i=1}^n \frac{1}{x_i} = \sum_{i=1}^n \frac{1}{x_i} = \sum_{i=1}^n \frac{1}{x_i} = \sum_{i=1}^n \frac{1}{x_i}$$

$$\frac{1}{x} = \frac{1}{x} = \frac{1}{x} = \frac{1}{x}$$

where the term on the right is the logarithmic derivative. For small x , this reduces to

$$-\frac{1}{x} = \frac{1}{x} = \frac{1}{x} = \frac{1}{x}$$

and the equation is also valid as $x \rightarrow \infty$ (see also (7.1) for the asymptotic behavior of $\frac{1}{x}$). In our case, the asymptotic behavior of the function $f(x)$ is given by the first equation. This is the main result of the paper. The proof is given in the appendix.

$$f(x) = \frac{1}{x} = \frac{1}{x} = \frac{1}{x} = \frac{1}{x}$$

is assumed. This gives the asymptotic behavior, and the relation for $f(x)$ and $f'(x)$ is obtained. The asymptotic behavior of $f(x)$ is given by the first equation. This is the main result of the paper. The proof is given in the appendix.

the results of the two theories. For the tension, rigidity, and plate thickness employed in the device, the solutions predict $\omega_i = 100$ and $\omega_r = 1000$. The approximation is necessary because the plotted data must be extrapolated to include the values of tension specified. These results show correlation within an order of magnitude of those predicted in Chapter V. ($\omega_r =$, ω_i). Most of flutter investigation has been restricted to determining the onset of flutter and methods for avoiding its occurrence. Again using our parameters in figure 10 of reference 18, flutter is predicted to occur when the tension corresponds to making $v_m + = v-c$. This is surprisingly consistent with the previous results. The predicted flutter frequency under these conditions is on the order of $20\omega_0$ where ω_0 equals the natural plate frequency neglecting tension. The previous results predict $\omega_f = 10\omega_0$.

There is considerable agreement between the two results, in spite of the difference in boundary conditions.

the results of the two theories. For the common, regular, and
 plate thicknesses employed in the study, the solution predicts $\gamma = 100$
 and $\mu = 1000$. The approximation is slightly better than
 stated and may be extrapolated to include the values of γ
 also specified. These results show agreement within an order
 of magnitude of those predicted in Figure 1. $\gamma = 100$
 and $\mu = 1000$ of linear interaction are then, corrected
 to determine the onset of linear and non-linear interaction.
 Again using the parameters in Figure 1 of reference
 18, Figure 18 predicts an onset of linear interaction at
 $\gamma = 4 \times 10^{-4}$. This is surprisingly constant with the
 values reported. The predicted linear interaction onset curve
 also is in the order of 10^4 when γ equals the onset value
 of linear interaction. The previous results predict

$$\gamma = 100$$

There is considerable agreement between the two results.
 in order of the difference in density prediction.

Appendix B

The previously described experiment was constructed. However, the improved end conditions to lessen the flow disturbance were mechanically unweildly. They did not provide the firm connection desired. Therefore, no further results of significance can be reported.

1. C. B. Morgan, A. H. Fairbridge, W. J. Shaw, E. J. J. Smith, "Control Policy of Automatic Turbidity and Flow Regulation of Flumes," *ASCE Trans.*, Washington, D. C., 1955.
2. E. J. Gagliardi, E. Smith, T. C. Gifford, "Automatic Control of Turbidity in Flumes," *ASCE Trans.*, Washington, D. C., 1955.
3. E. E. Kipping, "Automatic Control of Turbidity in Flumes," *ASCE Trans.*, Washington, D. C., 1955.
4. E. E. Kipping, "Automatic Control of Turbidity in Flumes," *ASCE Trans.*, Washington, D. C., 1955.
5. E. Kipping, "Automatic Control of Turbidity in Flumes," *ASCE Trans.*, Washington, D. C., 1955.
6. E. E. Kipping, "Automatic Control of Turbidity in Flumes," *ASCE Trans.*, Washington, D. C., 1955.
7. E. E. Kipping, "Automatic Control of Turbidity in Flumes," *ASCE Trans.*, Washington, D. C., 1955.
8. E. E. Kipping, "Automatic Control of Turbidity in Flumes," *ASCE Trans.*, Washington, D. C., 1955.
9. E. E. Kipping, "Automatic Control of Turbidity in Flumes," *ASCE Trans.*, Washington, D. C., 1955.
10. E. E. Kipping, "Automatic Control of Turbidity in Flumes," *ASCE Trans.*, Washington, D. C., 1955.

The previously listed accounts are summarized below:

BIBLIOGRAPHY

1. T. R. Brogan, A. R. Kantrowitz, R. J. Rosa, Z. J. J. Stekly, "Progress in MHD Power Generation," Second Symposium on the Engineering Aspects of Magnetohydrodynamics, Philadelphia, Pennsylvania, 1961, edited by C. Mannel and N. W. Mather (Columbia University Press, New York, 1962)
2. T. Theodorsen, "General Theory of Aerodynamic Stability and the Mechanism of Flutter," NACA R496, Washington, D. C. 1935.
3. R. L. Bisplinghoff, H. Ashley, R. L. Halfman, Aeroelasticity Addison-Wesley Publishing Co., Reading, Massachusetts, 1955.
4. P. S. Eagleson, Noutsopoulos, G. K., J. W. Daily, "The Nature of Self Excitation in the Flow Induced Vibration of Flat Plates," Trans., ASME, Journal of Basic Engineering, 1964.
5. P. Leehey, "Sonar Self-Noise," Seminar held on January 4, 1966, at Massachusetts Institute of Technology.
6. R. H. Lyon, "Response of Strings to Random Noise Fields" JASA, 28, No. 3, May 1956.
7. J. P. Den Hertog, Mechanical Vibrations, McGraw Hill Book Co. Inc., New York, 1956.
8. J. R. Melcher, Field Coupled Surface Waves, A Comparative Study of Surface Coupled EHD and MHD Systems, MIT Press, Cambridge, Massachusetts, 1963.
9. F. D. Ketterer, Electromechanical Streaming Interactions, Ph.D. Thesis, Dept. of Elect. Eng., MIT, 1965.
10. Dugundji, J. Dowell, E., and Perkin, B., "Subsonic Flutter of Panels on Continuous Elastic Foundations," AIAA Journal, Col. 1, No. 5, 1963.

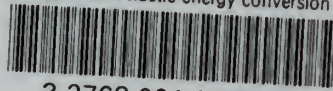
BIBLIOGRAPHY CONTINUED

11. Bers, A., and Briggs, R. "Criteria for Determining Absolute Instabilities and Distinguishing Between Amplifying Waves and Evanescent Waves," QPR No. 71, RLE, MIT, October 16, 1963.
12. Mills, J. D., A Computer Display System for Analyzing Polynomial Type Dispersion Relations, M.S. Thesis, Department of Electrical Engineering, MIT, 1965.
13. Louisell, W. H., "Coupled Mode and Parametric Electronics", John Wiley & Sons, Inc., New York, 1966.
14. Briggs, John M., Introduction to Structural Dynamics, McGraw-Hill Book Company, New York, 1964.
15. Shapiro, A. G., The Dynamics and Thermodynamics of Compressible Fluid Flow, The Ronald Press Company, New York, 1953.
16. Mercer, Albert G., "Turbulent Boundary Layer Flow over a Flat Plate Vibrating With Transverse Standing Waves," St. Anthony Falls Hydraulic Laboratory Report No. 41, Series B., Minneapolis, Minnesota, September 1962.
17. Fraize, W. F., Investigation of the Periodic Forced Motion of a Cantilever Fin in a Flowing Stream, Sc.D. Thesis, Department of Mechanical Engineering, 1964.
18. Dugundji, John, "Theoretical Considerations of Panel Flutter at High Supersonic Mach Numbers", AFOSR Report 65-1907, August 1965.

11. Serre, J.-P. and M. Artin, "On the Brauer group of a curve over a finite field", *Journal of the American Mathematical Society*, 1974, 1, 1-16.
12. Serre, J.-P., "On the Brauer group of a curve over a finite field", *Journal of the American Mathematical Society*, 1974, 1, 1-16.
13. Serre, J.-P., "On the Brauer group of a curve over a finite field", *Journal of the American Mathematical Society*, 1974, 1, 1-16.
14. Serre, J.-P., "On the Brauer group of a curve over a finite field", *Journal of the American Mathematical Society*, 1974, 1, 1-16.
15. Serre, J.-P., "On the Brauer group of a curve over a finite field", *Journal of the American Mathematical Society*, 1974, 1, 1-16.
16. Serre, J.-P., "On the Brauer group of a curve over a finite field", *Journal of the American Mathematical Society*, 1974, 1, 1-16.
17. Serre, J.-P., "On the Brauer group of a curve over a finite field", *Journal of the American Mathematical Society*, 1974, 1, 1-16.
18. Serre, J.-P., "On the Brauer group of a curve over a finite field", *Journal of the American Mathematical Society*, 1974, 1, 1-16.
19. Serre, J.-P., "On the Brauer group of a curve over a finite field", *Journal of the American Mathematical Society*, 1974, 1, 1-16.
20. Serre, J.-P., "On the Brauer group of a curve over a finite field", *Journal of the American Mathematical Society*, 1974, 1, 1-16.

thesB858

A magnetoaeroelastic energy conversion s



3 2768 001 01858 3

DUDLEY KNOX LIBRARY